Nanoscale Advances

Accepted Manuscript

This article can be cited before page numbers have been issued, to do this please use: S. Umapathy and I. Pan, *Nanoscale Adv.*, 2025, DOI: 10.1039/D4NA00644E.

ROYAL SOCIETY OF CHEMISTRY

rsc.li/nanoscale-advances

View Article Online
DOI: 10.1039/D4NA00644E

Title: Glucose Reduced Nano-Se Mitigate Cu-Induced ROS by Upregulating Antioxidant Gene in Zebrafish Larvae

Author Name: Suganiya Umapathy and Ieshita Pan*

Address: Institute of Biotechnology, Department of Medical Biotechnology, Saveetha School of Engineering, Saveetha Institute of Medical and Technical Sciences, Thandalam, Chennai, 602 105, Tamil Nadu, India

***Correspondence:** bony.iesk@gmail.com; ieshitapan.sse@saveetha.com

Keywords: Oxidative Stress, Nano-Se, Zebrafish Model, Antioxidant, Cognitive, Neurodegenerative Diseases

View Article Online
DOI: 10.1039/D4NA00644E

ABSTRACT

This study compares the therapeutic efficiency of bovine serum albumin-stabilized selenium nanoparticles in reducing oxidative stress and improving cellular health. The nanoparticles were synthesized using mussel-extracted selenium with two reducing agents: D-glucose and orange. Inductively coupled plasma-optical emission spectroscopy and X-ray Diffraction analyses confirmed the presence of selenium. The reducing agent and duration influenced the nanoparticle size. Reduction with D-glucose for 1 hour revealed that the particles exhibited an average size of 10 nm. Copper sulphate-induced malformations like yolk sac and pericardial edema were observed with 25 µg/ml of orange-reduced nanoparticles, while D-glucose-reduced nanoparticles mitigated these malformations at 25 µg/ml. Treatment with stabilized Se-NPs reduced with D-glucose for 30 minutes showed 33% dose-dependent radical scavenging activities, upregulated approximately 2-fold of superoxide dismutase, catalase, glutathione reductase, and glutathione peroxidase encoding genes, restored homeostasis by decreasing lipid peroxidation (27.32 nmol/mg/ml) and nitric oxide levels (6.71 µM). They also had the potential to restore cognitive properties like larval movement (93.40 m) without altering larval behaviour. Live cell imaging indicated a significant decrease in cellular reactive oxygen species and lipid peroxidation levels in the gut and liver. These findings suggest that Se-NPs reduced for 30 minutes with D-glucose are promising candidates for oxidative stress-induced neurodegeneration.

INTRODUCTION

Mitochondria are dynamic, membrane-bound organelles that play a pivotal role in orchestrating cellular energy production in almost all eukaryotic cells. They are central to sustaining life by generating the ATP required for various cellular functions and regulating several metabolic processes, including redox homeostasis, calcium signaling, and cellular apoptosis[1,2]. Mitochondria are one of the most crucial organelles involved in the structure and function of neuronal networks in the brain. Disruption of mitochondrial homeostasis can directly progressoxidative damage, leading to neurodegeneration[3]. Major contributors to mitochondrial dysfunctionare mitochondrial fission, fusion, and mitophagy, leading to neurodegenerative diseases including Alzheimer's Disease (AD), Parkinson's Disease (PD), Amyotrophic Lateral Sclerosis (ALS), and Prion diseases etc[4,5]. Excessive fusion leads to the formation of elongated mitochondrial tubules, while increased fission initiates the fragmentation of mitochondria[6]. These events trigger oxidative stress, halt the production of energy, and cause abnormal signaling in cellular pathways[7]. Reactive oxygen species (ROS) can be both beneficial and detrimental to human health. Generally, ROS contributes to several redox-regulating processes within cells to maintain cellular homeostasis. However, overproduction and accumulation of ROS lead to oxidative stress, damaging cell structures and causing various diseases[8,9]. Under both healthy and pathological situations, mitochondria are the primary source of ROS. Superoxide and hydroxyl radicals are the primary oxygen-free radicals[10]. Cellular respiration like lipoxygenases (LOX) and cyclooxygenases (COX), produces superoxide anion radicals[11]. The pathophysiology of chronic illnesses like cancer, diabetes, neurodegenerative diseases, and cardiovascular diseases is heavily influenced by oxidative stress. Oxidative stress increases the levels of pro-oxidant factors, leading to structural alterations in mitochondrial DNA and functional alterations by aberrant gene expression[12].

Nanotechnology has received significant attention due to the well-established fact that its combination with biotechnology creates a platform with enormous potential and significance in terms of its variety of applications[13]. Different kinds of nanoparticles (NPs)

View Article Online
DOI: 10.1039/D4NA00644E

can be formulated to maximize their functions; these include semiconductor, metal, metal oxide, organic, and inorganic NPs. Semiconductor nanoparticles, such as quantum dots, are used in controlled drug release due to their responsive optical and electronic properties[14]. Treatment with metal oxide NP i.e., CeO_2-NP decreased post-injury neuronal death anddamage while improving CAT, SOD activity levels, and glutathione:glutathione-disulfide ratios notably[15]. Silver NP efficiently inhibited lipid peroxidation (LPO)by scavenging ROS, showing their antioxidant effectiveness[16].Organic NPs, such as liposomes, enhance drug bioavailability by encapsulating hydrophobic drugs[17], while inorganic NPs offer stability and targeted delivery[18]. Diverse approaches can be implemented in the production of NPs, including green synthesis and conventional chemical synthesis[19]. Selenium (Se) is an essential micronutrient that is involved in the proper functioning of all organisms. It is a cofactor of many enzymes including glutathione peroxidase and thioredoxin reductase. Selenoproteins, such as selenocysteine and selenomethionine are crucial forms naturally present in prokaryotes and eukaryotes. Se is an effective radical scavenging agent against oxidative stress[20]. Deficiency of Se can lead to chronic diseases such as diabetes, cardiovascular disease, obesity, respiratory diseases, neurodegenerative diseases, and cancer [21]. To overcome this, inorganic forms of Se (selenite and selenate) are being used as dietary supplementation[20]. Selenium nanoparticles (Se-NPs) are known to have high bioavailability and a low toxicity profile[22–24]. They can reduce the accumulation of free radicals and prevent oxidative stress[25]. One of the major contributors to free radicals is an increase in NO and malondialdehyde (MDA) levels, which triggers LPO[26,27]. Copper NP triggers oxidative stress by elevating LPO while disrupting antioxidantenzymes[28]. Se-NPs significantly reduceMDA levels and restore antioxidant enzyme activity[29,30]. Se-NPs potentially eliminated oxidative stress induced by streptozotocin by decreasing the LPO and NO levels in the pancreas[31].Therefore, nano-Seplaysa crucial role as an antioxidant defence system[32].Moreover, Se-NPs can cross the blood-brain barriershowing their potential in modulating inflammation and brain-related diseases[33,34].Some of the emerging *in vitro* and *in vivo*studies using PC12 cell lines and rat modelshighlighted the therapeutic efficacy of Se-NPs in mitigating oxidative stress and neurodegenerative diseases such as AD and PD[35–38]. Though Se-NPs have many therapeutic benefits, most were chemically synthesized using sodium selenite which may induce mild toxic effects[39–42].

This study hypothesizes that Se-NPs could mitigate copper-induced neurotoxicity through multiple mechanisms, including reducing oxidative stress, restoring mitochondrial function, and reactivating antioxidant enzyme systems. Copper-induced toxicity is known to generate excessive reactive oxygen species (ROS), leading to lipid peroxidation, mitochondrial dysfunction, and inhibition of key enzymes such as SOD, CAT, GSH, GPx, and AChE. By counteracting these effects, Se-NPs hold promise as a therapeutic strategy for addressing oxidative stress-related neurodegenerative conditions. In this study, we synthesized Se-NPs using selenium obtained from mussels. Mussels are known for their unique ability to bioaccumulate selenium, a micronutrient with potential antioxidant and health benefits.We employedvarious reducing agents, namely D-glucose and orange with BSA as a stabilizer. These reducing agents were applied at two different time intervals to assess their efficiency in reducing the size and preventing aggregation of the nanoparticles. The synthesized Se-NPs were characterized and subsequently tested for their antioxidant and neuroprotective properties against copper sulfate ($CuSO_4$)-induced stress *in vivo* in zebrafish larvae. The study aims to evaluate the potential of Se-NPs in restoring enzymatic activity and neurotransmitter function disrupted by copper toxicity while highlighting their broader applications in mitigating oxidative stress-induced damage.

RESULTS AND DISCUSSION

View Article Online
DOI: 10.1039/D4NA00644E

Synthesis and Characterization of Mussels Extracted Se

Different extraction methodssuch as 0.8% saline and Tris-HCl buffer (pH-7.4)extraction methods were utilized to determine the most suitable method for extractingSe from mussels. Results from ICP-OES showedsharp peak at 196.03 nm with a concentration of 0.93 mg/L for the saline extraction method and 0.51 mg/L for the buffer extraction method **(Fig. 1a,b)**. Similarly, a study conducted by Tyburska *et al*. also reported a peak at 196.03 forselenium[43]. For Se extracted using a saline method, the XRD data revealed peaks at 26.51°, 31.58°, 45.33°, 56.31°, 66.13°, and 75.16° angles corresponding to the planes (100), (110), (111), (112), (210), and (113), respectively. The nature was observed to be 85% crystalline and 15% amorphous. Conversely, Se extracted using the buffer method showed peaks at 22.16° and 26.77°, corresponding to the planes (100) and (110), respectively **(Fig. 1c,d)**.The nature was observed to be 70% crystalline and 30% amorphous.Astudy conducted in 2019, by Hassanien *et al*. focused on dye degradation and also observed XRD peaks aligningwith the corresponding planes for Se-NPsconfirming the presence of Se[44].

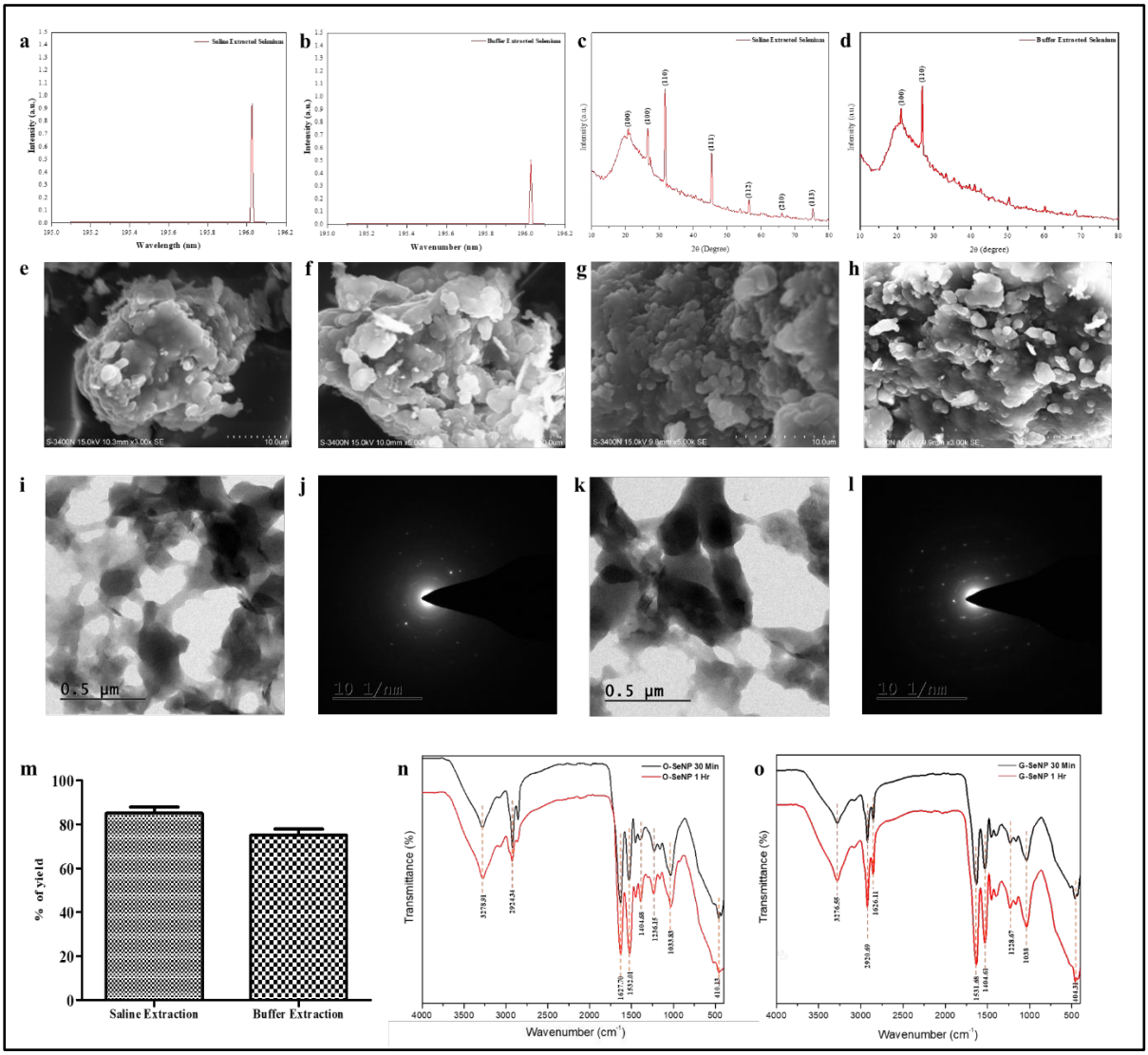

Fig. 1 Synthesis and Characterization of Se extracted from mussel and Se-NPs: ICP-OES(a) Saline extracted Se; (b) Buffer extracted Se; XRD analysis (c) Saline extracted Se; (d) Buffer extracted Se; SEM (e-f) stabilized Se-NPs reduced for 30 minutes and 1hour with D-glucose; (g-h) stabilized Se-NPs reduced for 30 minutes and 1hour with orange; TEM and SAED (i-j) stabilized Se-NPs reduced for 30 minutes with D-

View Article Online
DOI: 10.1039/D4NA00644E

Glucose;(k-l) stabilized Se-NPs reduced for 30 minutes with orange. Yield (m) Percentage of Se yield. FTIR (n) stabilized Se-NPs reduced for 30 minutes and 1 hour with D-glucose; (o) stabilized Se-NPs reduced for 30 minutes and 1 hour with orange peel extract.

Synthesis and Characterization of Mussel extracted Se-NPs

Se was reduced using D-glucose and orange peel extract to synthesize Se-NPs. The reduction process was carried out at two different time periods (30 minutes and 1 hour) to determine the efficiency of reducing agents and were stabilized using BSA to prevent aggregation.A study by El Badawy *etal*. reported that stabilization kinetics impact the aggregation pattern of nanoparticles[45].SEM imaging at $5x10^{-3}$ magnification was done to determine the morphology of Se-NPs. SEM results showed that the nanoparticles revealed a near-spherical shape for both non-stabilized and stabilized Se-NPs. Compared to non-stabilized Se-NPs, stabilized nanoparticles exhibited less aggregation. The mean area and length of the nanoparticles were calculated using ImageJ software, which was found to be 20±3 and 10±3 nm for stabilized Se-NPs reduced with D-glucose for 30 minutes and 1 hour **(Fig. 1e,f)**. On the contrary, the size of non-stabilized Se-NPs reduced with orange for 30 minutes and 1 hour was observed to be 33±6 and 29±7 nm **(Supplementary Fig 1a,b)**. In 2016, a study by Nie *et al*. on the synthesis of highly uniform Se-NPs using glucose as a reductant reported that the nanoparticles were spherical and were about 240 nm in size[46].Glucose-reduced Se-NPs were spherical with a size ranging from 280-295 nm[46]. Se-NPs reduced with orange were reported to be spherical with a size range of 16–95 nm[47].Similarly, the size of stabilized Se-NPs reduced with orange peel extract for 30 minutes and 1 hour was observed to be 19±4 and 18±7 nm**(Fig. 1g,h)**, respectively, while non-stabilized Se-NPs reduced with orange peel extract for 30 minutes and 1 hour were found to be 29±8 and 26±9 nm**(Supplementary Fig 1c,d)**, respectively. A study on the green synthesis of Se-NPsusing orange peel by Salem *et al*. reported that the nanoparticles were spherical and size ranged between 16-95 nm[47]. Se-NPs synthesized from mussel-extracted Se were found to be similar in shape and were reduced better with D-glucose. Based on the size reduction and aggregate formation it was assumed that the stabilized reduction process produced better nanoparticleswhich can be an advantage to pass through the blood-brain barrier.TEM imaging confirms the near-spherical shape. The mean area of Se-NPs reduced with D-glucose was 23.95±6.18 nm **(Fig.1i)** and Se-NPs reduced with orange was 53.50±21.96 nm **(Fig. 1k)**. A study by Van der Horst *et al.* on electrochemical sensor applications using bismuth-silver nanoparticles showed that TEM of silver nanoparticles ranged between 10 and 20 nm with spherical shapes and accompanied with some aggregates[48]. SAED pattern showed concentric diffraction rings interspersed with discrete spots, which are characteristic of a polycrystalline material with localized crystalline domains. This indicates that the sample contains multiple crystallites with varying orientations, contributing to the ring formation **(Fig. 1j&l)**. Particle size analysis showed that Se-NPs reduced with D-glucose and orange were monodispersed with a size of 310.1±73.2 nm and 378±102.1 nm under refractive index 1.59 **(Supplementary Fig 1e)**. Zeta potential was measured at -1.2 mV and 0.4 mV, indicating the particles have a very low surface charge or are nearly neutral, which tend to aggregate. The sharp peak implies a uniform distribution of zeta potential values **(Supplementary Fig 1f,g)**. Similar patterns were observed in a study by Bhattacharyya *et al.* on the one-pot fabrication of silver nanoparticles[49].

The total yield of Se was observed to be approximately 10% higher in the 0.8% saline extraction method, compared to the buffer extraction method **(Fig. 1m)**. This percentage was calculated based on the dry weight of the extracted selenium in milligrams. The chemical attributes of the stabilized Se-NPs were determined using FTIR. The smooth and sharp peaks

View Article Online
DOI: 10.1039/D4NA00644E

observed were at 3276.55-3278.35 cm^{-1}(medium, sharp C-H stretching alkene), 2920.69-2850.78 cm^{-1}(medium, sharp C-H stretching alkane), 1626.11-1626.07 cm^{-1}(medium, C=C stretching di-substituted alkene), 1531.68-1530.69 cm^{-1} (strong, N-O stretching nitro-compound), 1404.61-1402.19cm^{-1} (strong, S=O stretching sulfonyl chloride), 1228.67-1228.37 cm^{-1} (strong, C-O stretching alkyl aryl ether), 1038-1035.12 cm^{-1}(strong, S=O stretching sulfoxide), and 518.39-404.31 cm^{-1} (strong, metal-ligand stretching) for stabilized Se-NPs reduced for 30 minutes and 1 hour with D-glucose **(Fig. 1n)**. Stabilized Se-NPs reduced for 30 minutes and 1 hour with orange showed peaks at 3278.91-3273.23cm^{-1}(medium, sharp C-H stretching alkene), 2924.34-2851.30cm^{-1}(medium, sharp C-H stretching alkane), 1627.70-1627.66cm^{-1}(medium, C=C stretching di-substituted alkene), 1532.01-1515.51cm^{-1}(strong, N-O stretching nitro-compound), 1404.68-1392.67 cm^{-1}(strong, S=O stretching sulfonyl chloride), 1236.15-1228.28cm^{-1}(strong, C-O stretching alkyl aryl ether), 1033.83-1031.98 cm^{-1}(strong, S=O stretching sulfoxide), and 472.40-410.13 cm^{-1}(strong, metal-ligand stretching)**(Fig. 1o)**. The obtained peaks indicated the presence of metal, stabilizer, and the reducing agents used **(Supplementary Table 1)**. The time of reduction and variation in the reducing agent did not significantly affect the position of functional groupsin the nano-Se. Similar peaks were observed in the study reported by Alagesan & Venugopal for green-synthesized Se-NPs[50].

Developmental Toxicity Assessment

The developmental toxicity assessment of Se-NPs (5-25µg/ml) was conducted using zebrafish embryos. Concentration was selected based on a previously reported studythat obtained a similar model and showed regulated biological effects without exacerbating the system[51].In the control group, no abnormal morphological changes were observed. Groups treated with stabilized Se-NPs reduced with D-glucose for 30 minutes and 1 hour (5-25µg/ml) for 0-72 hpf showed no malformation, compared to the stress-exposed group which showed malformations like pericardial edema (PSE) and yolk sac edema (YSE)**(Fig. 2a,b)**. On the other hand, groups treated with stabilized Se-NPs(5-20 µg/ml)reduced with orange for 30 minutes and 1 hour showed no malformations, while 25 µg/ml showed malformations like bent spine (BS) and YSE **(Fig. 2c,d)**. Compared to stabilized Se-NPs reduced with orange for 30 minutes and 1 hour, stabilized nano-Se reduced with D-glucose for 30 minutes and 1 hour showed a higher survival rate at 96 hpf, reducing $CuSO_4$-induced stress **(Fig. 2a1-d1)**. Bulk selenium showed lesser survival rate compared to nano-selenium **(Supplementary Fig 2)**.A previous study on green synthesized Se-NPsand their toxicity profile by Kalishwaralal *et al*. reported that at 15-25µg/ml, malformations like tail malformation and PSE were observed[51].Exposure to hydrogen peroxide (5 mM) until 120 hours post-fertilization induced stress, significantly reducing the survival rate of zebrafish embryos and larvae[52].Furthermore,zebrafish embryos and larvae treated with BSA-synthesized Se-NPs at concentrations of 20-25 µg/ml showed mortality[51]. Therefore, mussel-extracted Se-NPs reduced with glucose can be a potential alternative source with lower toxicities.

View Article Online
DOI: 10.1039/D4NA00644E

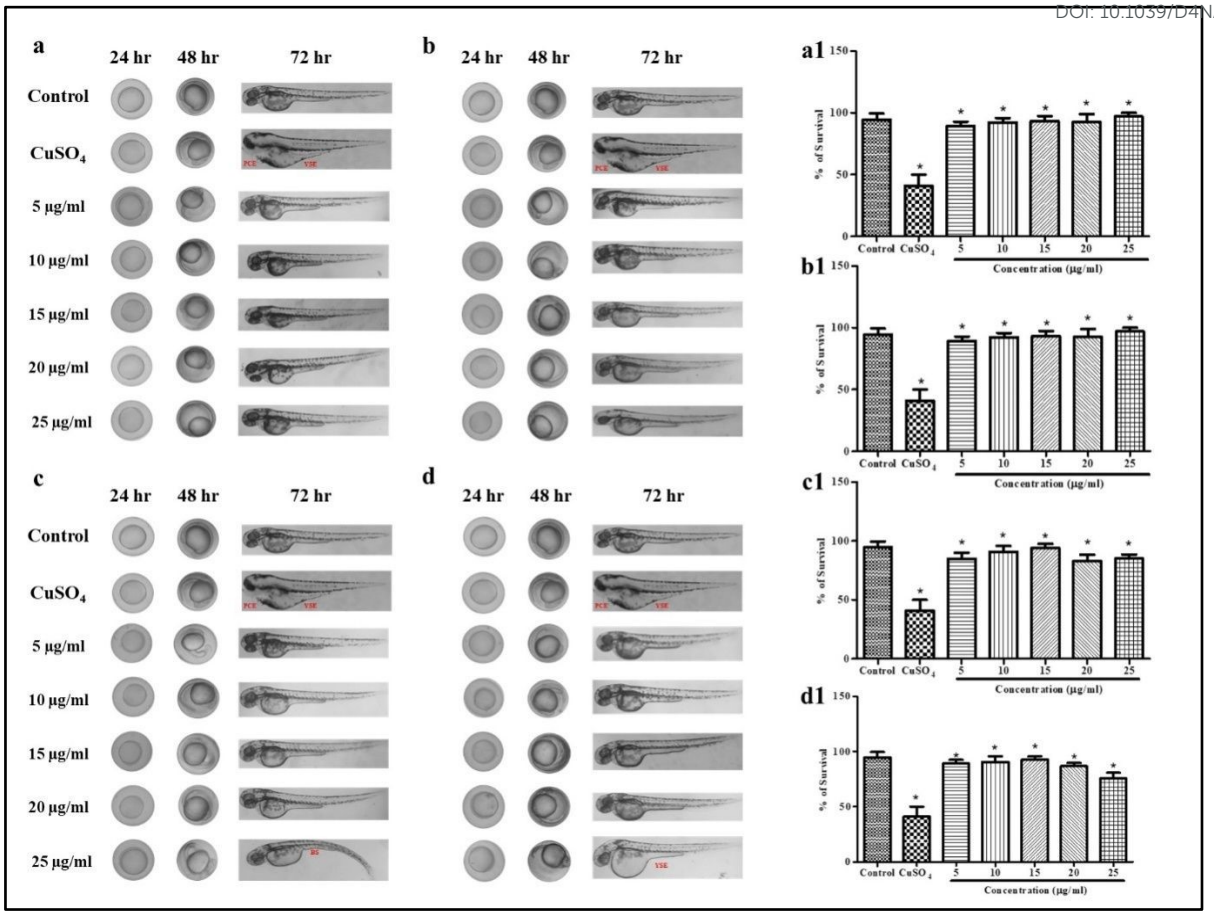

Fig.2*In Vivo* Developmental Toxicity Analysis in zebrafish embryos and larvae representing, Control group; Stress group ($CuSO_4$-induced stress); and Stabilized Se-NPs (5-25 µg/ml) treatment group. (a-b) stabilized Se-NPsreduced with D-glucose for 30 minutes and 1 hour, (c-d) stabilized Se-NPsreduced with orange peel extract for 30 minutes and 1hour.Survival rate (a1-b1) stabilized Se-NPsreduced with D-glucose for 30 minutes and 1 hour, (c1-d1) stabilized Se-NPsreduced with orange peel extract for 30 minutes and 1hour.The data were considered significant ($p < 0.05$) and marked by the symbol "*".

In Vitro Antioxidant Analysis of Stabilized Se-NPs

a) DPPH Scavenging Assay

The DPPH scavenging assay was conducted to evaluate the ROS scavenging activity. As a positive control, ascorbic acid (AsA) exhibited 50% scavenging activity. Stabilized Se-NPs reduced with D-glucose for 30 minutesand 1 hour showed concentration-dependent DPPH scavenging activity. The highest scavenging activity was observed at a concentration of 25µg/ml with 33.20% and 29.29% inhibition**(Fig. 3a,b).** Stabilized Se-NPs reduced with orange peel extract for 30 minutes and 1 hour,exhibited radical scavenging activity at all concentrations, but the highest activity was seen at a concentration of 15 µg/ml with 18.62% inhibition.Additionally, the stabilized nano-Se reduced with orange peel extract for 1 hour showed 17.79% radical scavenging activity ($p < 0.05$)**(Fig. 3c,d)**. The IC50 value was observed to be 20.59µg/ml.Therefore, stabilized Se-NPs were found to be efficient DPPH scavengers.In a 2017 study reported by Vyas & Rana, it was shown that aloe extract combined with Se-NPs had higher DPPH scavenging activity thanaloe extract alone[53], indicating the significant potential of Se-NPs as an antioxidant. Conversely, astudy by Zhai *et al.* reported that chitosan-reduced Se-NPs exhibited ~60% higher scavenging activity in the ABTS assay compared to the DPPH assay[54].

View Article Online
DOI: 10.1039/D4NA00644E

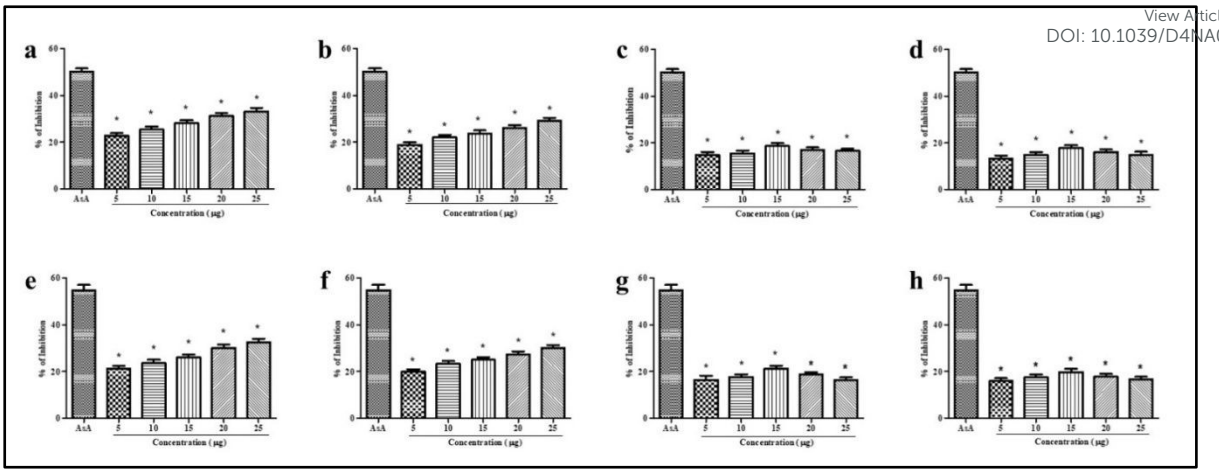

Fig. 3 ***In Vitro*** **Antioxidant Activity:** DPPH assay of (a-b) stabilized Se-NPs reduced with D-glucose for 30 minutes and 1 hour, (c-d) stabilized Se-NPsreduced with orange peel extract for 30 minutes and 1hour. ABTS assay of (e-f) stabilized Se-NPsreduced with D-glucose for 30 minutes and 1 hour, (g-h) stabilized Se-NPs reduced with orange peel extract for 30 minutes and 1hour. The data were considered significant ($p < 0.05$) and marked by the symbol "*".

b) ABTS Scavenging Assay

The ABTS scavenging assay was conducted to determine the ROS scavenging activity. Ascorbic acid (AsA)exhibited 55% scavenging activity, serving as a positive control. All stabilized Se-NPs reduced with D-glucose displayed concentration-dependent scavenging activity. However, the maximum activity was observedat 30 minutes and 1 hour, with percentages of 32.59% and 30.01% respectively, at a concentration of 25 µg/ml**(Fig. 3e,f)**.In another group, stabilized Se-NPs reduced with orange peel extract for 30 minutes and 1 hour, showed radical scavenging activity acrossall concentrations. The maximum inhibition was observed at a concentrationof 15 µg/ml ($p < 0.05$), for both 30 minutes(21.25%) and 1 hour (19.84%)**(Fig. 3g,h)**.The IC50 value corresponds to 16.86µg/ml, respectively. Vyas & Rana also noted that aloe extract combined with Se-NPsexhibited higher ABTS scavenging activity compared to aloe extract alone[53], suggesting theirpotential antioxidant properties.

In Vivo Enzymatic Assay of Stabilized Se-NPs

a) SOD Assay

SOD levels were determined using a homogenized sample of zebrafish larvae exposed to $CuSO_4$ followed by treatment with stabilized Se-NPs. In the $CuSO_4$ exposed group, SOD levels drastically decreased to 7.33 U/mg of protein (a 57% reduction), compared to the control (16.90 U/mg of protein). Stabilized Se-NPs reduced with D-glucose for 30 minutes and 1 hour,restored the enzyme levelsby more than 83%, producing SOD levels of 14.74 U/mg of protein and 14.11 U/mg of protein respectively at a concentration of 25 µg/ml, showing a concentration-dependent enhancement in enzyme activity **(Fig. 4a,b)**. Alternatively, at 15 µg/ml concentration, stabilized Se-NPs reduced with orange for 30 minutes and 1 hour showed total SOD levels of 12.15 U/mg of protein and 11.84 U/mg of protein, approximately 72% and 70% restoration compared to the control.However, at a concentration of 25 µg/ml, the pattern was reversed with a decrease in SOD activity to 10.24 U/mg of protein and 9.90 U/mg of protein **(Supplementary Fig 3a,b)**, respectively. In 2023, a study by Naz *et al*. showed that $CuSO_4$decreased SOD levels[55]. However, Khan *et al*. in 2022 reported that SOD enzyme levels can be elevated upon Se-NPs application[56].

View Article Online
DOI: 10.1039/D4NA00644E

b) CAT Assay

CAT levels were assessed using a standardized sample of zebrafish larvae exposed to $CuSO_4$ followed by treatment with stabilized Se-NPs. In the group exposed to $CuSO_4$, there was a significant decrease in CAT levels specifically 2.49 µmol/mg of protein, compared to the controlgroup (8.72 µmol/mg of protein). Zebrafish larvae exposed to $CuSO_4$and treated with stabilized Se-NPs combined with D-glucose for 30 minutes and 1 hour exhibited a dose-dependent increase in total CAT levels of 7.33 µmol/mg and 7.16 µmol/mg of protein at a concentration of 25 µg/ml **(Fig. 4c,d)**. While treated with15 µg/ml stabilized Se-NPs reduced with orange for 30 minutes and 1 hour, the total CAT concentration only increased to 5.64µmol/mg and 5.67 µmol/mg respectively.However,ata concentration of 25 µg/ml,CAT activity decreasedto 4.59 µmol/mg and 4.55 µmol/mg of protein **(Supplementary Fig 3c,d)**, respectively. In 2023, Sariñana-Navarrete *et al*. stated that Se-NPsare effective antioxidants and maintain redox signaling by increasing the levels of the CAT enzyme[57].

c) Lipid Peroxidation Assays

In the$CuSO_4$ exposed stress group, significantly higher levels of MDA at 81.69 nmol/mg/ml were observed compared to the control group (17.09 nmol/mg/ml). When treating zebrafish larvae exposed to$CuSO_4$, stabilized Se-NPs reduced with D-glucose for 30 minutes and 1 hour at a concentration of 25 µg/ml significantly decreased the MDA levels by 27.32 and 33.84 nmol/mg/ml respectively **(Fig. 4e,f)**. Conversely,treatment with 15 µg/ml of stabilized Se-NPs reduced with orange peel extract for 30 minutes and 1 hour also reduced MDA levelsby approximately 38% and 33% compared to the $CuSO_4$ exposed stress group **(Supplementary Fig 3e,f)**. Liu *et al.* emphasized that copper nanoparticles induce oxidative stress by increasing LPO while disrupting SOD, CAT, and GPx enzyme activity[28]. A study by Lesnichaya *et al*. on carbon tetrachloride-inducedtoxicity in the liver reported that nano-Se neutralized the LPO levels[58].

d) Estimation of NO levels

NO levels were determined using the Griess reagent assay. $CuSO_4$-exposed zebrafish larvae showed a 1.98 times enhancementof NO levels (12.9 µM) compared to the control group (6.49 µM). Treatment with 25 µg/ml stabilized Se-NPs reduced with D-glucose for 30 minutes and 1 hour, resulted in a dose-dependent decrease in NO levels with approximately 6.71µM and 7.02 µM measured for the 30 minute and 1 hour treated groups, respectively **(Fig. 4g,h)**. Conversely, for $CuSO_4$ exposed-zebrafish larvae treated with 15 µg/ml of stabilized Se-NPs reduced with orange peel extract for 30 minutes and 1 hour, the measured NO levels were 8.87µM and 9.68µM **(Supplementary Fig 3g,h)**, respectively. Though both nanoparticles were effective in restoring NO levels upon treatment, stabilized Se-NPs reduced with D-glucose were found to be more efficient compared to orange-reduced nano-Se. A study by Anuse *et al*., reported that Se-NPs significantly reduced NO levels[59].

View Article Online
DOI: 10.1039/D4NA00644E

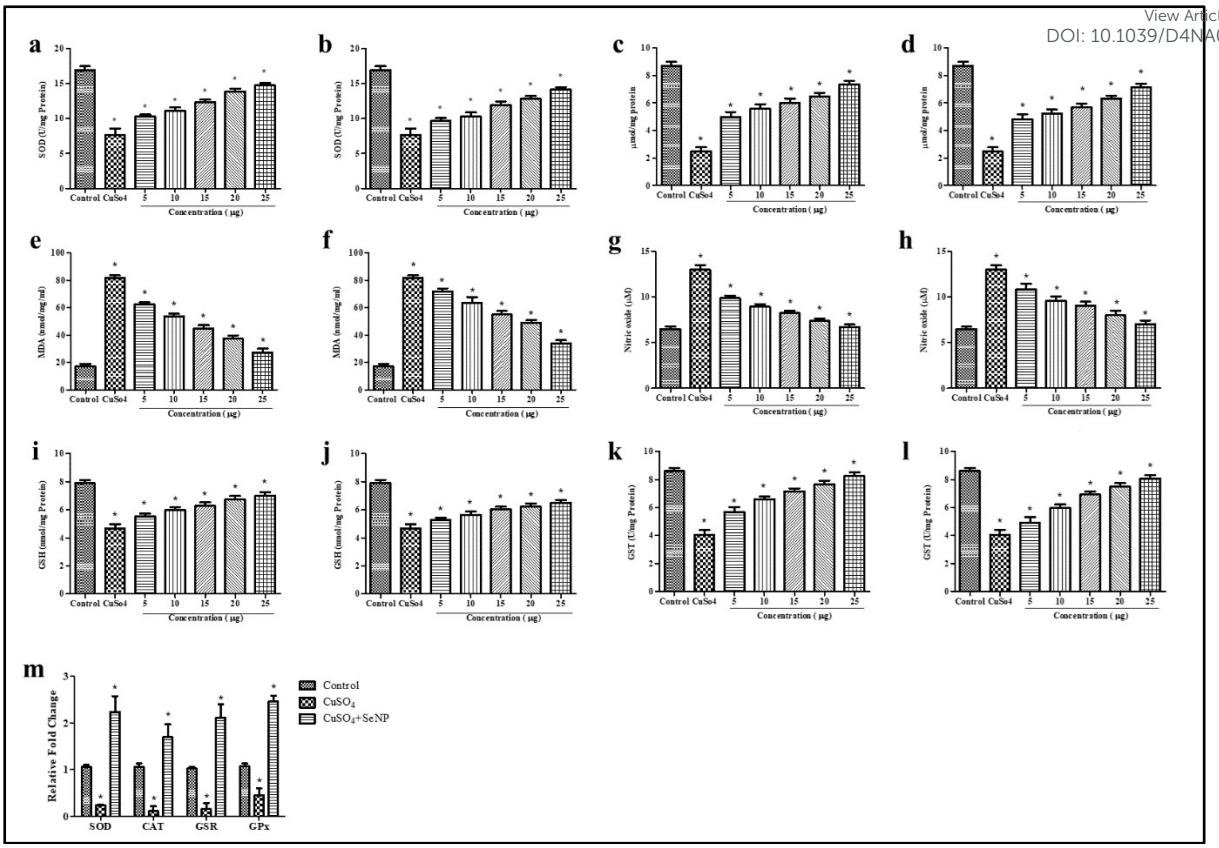

Fig. 4 *In Vivo*Antioxidant Activity of stabilized Se-NPs: SOD assay (a-b) reduced with D-glucose for 30 minutes and 1 hour, CAT assay (c-d) reduced with D-glucose for 30 minutes and 1 hour. LPO assay (e-f) reduced with D-glucose for 30 minutes and 1 hour.NO assay (g-h) reduced with D-glucose for 30 minutes and 1 hour.GSH assay (i-j) reduced with D-glucose for 30 minutes and 1 hour.GST assay (k-l) reduced with D-glucose for 30 minutes and 1 hour.RT-PCR (m) reduced with D-glucose for 30 minutes (25 µg/ml).The data were considered significant ($p < 0.05$) and marked by the symbol "*".

e) Estimation of GSH activity

The group exposed to $CuSO_4$ showed a significant reduction in GSH activity (4.67 nmol/mg protein) compared to the control group (7.89 nmol/mg protein). However, treatment with 25 µg/ml of stabilized nano-Sereduced with D-glucose for 30 minutes and 1 hour significantly increased GSH activity in $CuSO_4$-exposed zebrafish larvae. The GSH levelsincreased to 7.02 and 6.49 nmol/mg of protein, respectively **(Fig. 4i,j)**. A similar effect was observed when using stabilized Se-NPs reduced with orange peel extract at a concentration of15 µg/ml for 30 minutes and 1 hour. However, theGSH activity only increased to 6.17 and 5.72 nmol/mg of protein **(Supplementary Fig 3i,j)**. Therefore, stabilized nano-Se has potential antioxidant properties, which can reduce oxidative stress and protect cellular homeostasis. El-Borady *et al*. reported that Se-NPs increased GSH levels by decreasing ROS levels[60].

f) Estimation of GST activity

The $CuSO_4$ exposed group showed a significant reduction in GST activity (4.04 U/mg protein) compared to the control group (8.59 U/mg protein). Treatment with 25 µg/ml of stabilized Se-NPs reduced with D-glucose for 30 minutes and 1 hour significantly increased GST activity to approximately8.23 and 8.06 U/mg of protein respectively **(Fig. 4k,l)**. However, treatment with a concentration of 15 µg/ml of stabilized Se-NPs reduced with

orange peel extract for 30 minutes and 1 hour only restored GST activity up to 7.59 and 7.55 U/mg of protein **(Supplementary Fig 3k,l)**. This indicates the potentialof stabilized Se-NPs to reduce oxidative stress. Horky *et al*. study on the antioxidant activity of Se showed an improvement in GST activity by 25.3%[61].

Expression of Antioxidant Genes

Deficiency of selenium, a key component of antioxidant enzymes, modulates selenoproteins in turn triggering ROS production, leading to disruption of cellular homeostasis[62,63]. An antioxidant gene expression study was conducted in zebrafish larvae exposed to $CuSO_4$ and treated with stabilized Se-NPs reduced for 30 minutes and 1 hour with D-glucose as well as orange peel extract. Compared to the control group, the $CuSO_4$-induced stress group showed significant downregulation of SOD (0.2-fold), CAT (0.1-fold), glutathione-disulfide reductase (GSR) (0.1-fold), and Glutathione peroxidase (GPX) (0.4-fold) expression. In contrast, treatment with stabilized Se-NPs reduced for 30 minutes and 1 hour with D-glucose and stabilized Se-NPs reduced for 30 minutes and 1 hour with orange peel extract significantly ($p < 0.05$) upregulated the SOD (2.2-fold), CAT (1.7-fold), GSR (2.1-fold), and GPX (2.5-fold) expression, confirming its potential in influencing the expression of antioxidant genes by mitigating ROS**(Fig. 4m)**. This protective effect may likely be mediated through the nuclear factor erythroid 2-related factor 2 (NRF-2) pathway[64,65]. NRF-2 is a transcription factor that plays a pivotal role in cellular defense against oxidative stress. Under oxidative stress conditions, NRF-2 dissociates from Keap1 and binds to antioxidant response elements[66]. Real-time PCR studies reported by Handa *et al*.showed that upon utilization of selenium anti-oxidative enzymes encoding gene expression were elevated[67].

Localization of CellularROS

To evaluate the intracellular ROS level, DCFDA fluorescent staining was performedon zebrafish larvae (96 hours post fertilization; 96 hpf). The control group showed a mean fluorescent intensity (MFI) of 8.9.Zebrafish larvae exposed to $CuSO_4$had ROS levels of61.75 MFI.Whileoverall cellular ROS was detected in the larvae, maximum localization was found in the gut and liver regions.Treatmentwith stabilized Se-NPssignificantly ($p < 0.05$) reducedcellular ROS levels in$CuSO_4$-induced zebrafish larvae, compared to the untreated stress group **(Fig. 5a-d)**. The 25µg/ml stabilized Se-NPstreated with D-glucose for 30 minutes and 1 hourshowed lower ROS levels at concentrations of 10.1and 12.2 MFI **(Fig. 5a1,b1)**. In contrast, stabilized Se-NPs reduced with orange for 30 minutes and 1 hourshowed lower ROS levelsat concentrations of 15µg/ml with 17.67and 18.27 MFI **(Fig. 5c1,d1)**. Therefore, stabilized Se-NPs treated with D-glucose for 30 minutes could be a potential antioxidant therapeuticfor ROS-mediated neurodegeneration. Raju *et al*. conducted a similar protocol to assess the ROS levels in zebrafish larvae exposed to H_2O_2 stress, showing higher intensity in the stress group, compared to the treatment groups[68].

View Article Online
DOI: 10.1039/D4NA00644E

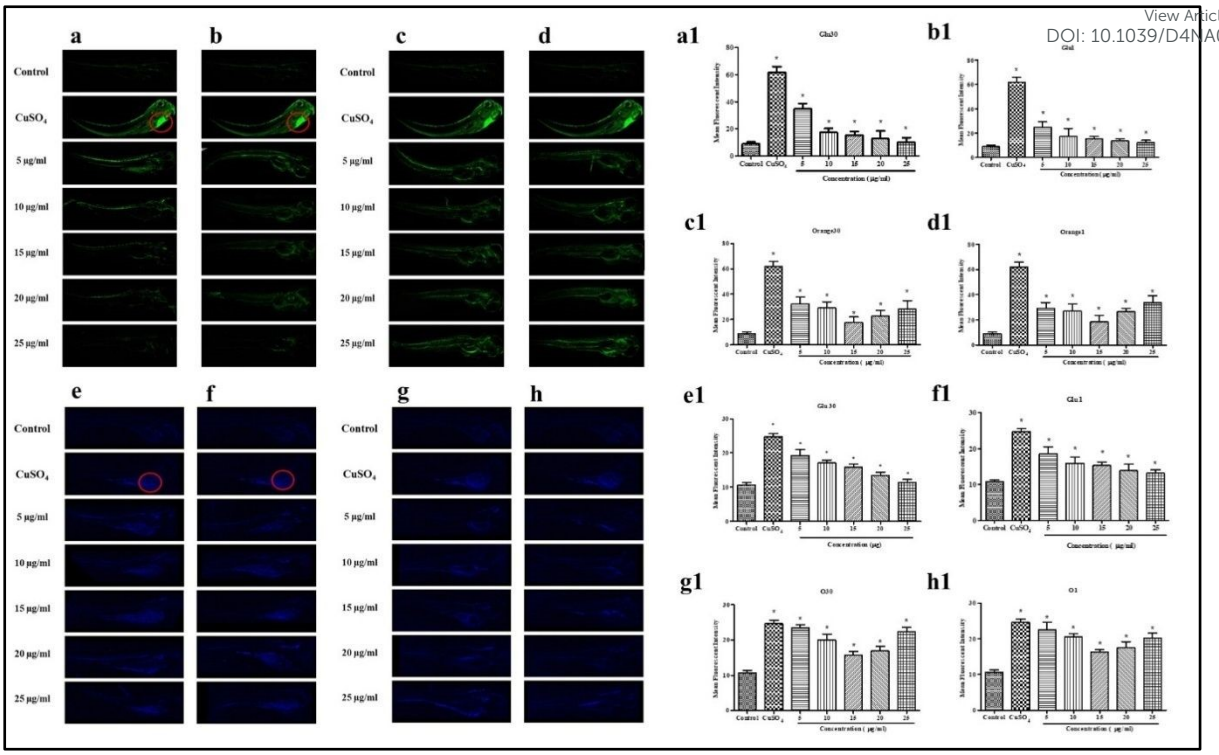

Fig. 5 Live Cell Imaging *In Vivo* in the Zebrafish Larvae Model at 96 HPF: DCFDA staining (a&a1) stabilized Se-NPs reduced with D-glucose for 30 minutes &MFI; (b&b1) stabilized Se-NPs reduced with D-glucose for 1 hour &MFI; (c&c1) stabilized Se-NPs reduced with orange peel extract for 30 minutes &MFI; (d&d1) stabilized Se-NPs reduced with orange peel extract for 1 hour &MFI. DPPP staining (e&e1) stabilized Se-NPs reduced with D-glucose for 30 minutes &MFI; (f&f1) stabilized Se-NPs reduced with D-glucose for 1 hour &MFI. (g&g1) stabilized Se-NPs reduced with orange peel extract for 30 minutes &MFI; (h&h1) stabilized Se-NPs reduced with orange peel extract for 1 hour &MFI. The data were considered significant ($p < 0.05$) and marked by the symbol "*".

Determination of Live Cell Lipid Peroxidation

To determine the LPO levels in zebrafish larvae (96 hpf), DPPP fluorescent staining was conducted. The control group exhibited lower LPO levels at 10.67 MFI. Zebrafish larvae exposed to $CuSO_4$showed increased LPO levels of 24.68 MFI.Treatment with stabilized Se-NPs significantly ($p < 0.05$) reduced LPO levels in$CuSO_4$-induced stress groupscompared to the untreated stress group **(Fig. 5e-h)**. However, treatment with stabilized Se-NPs reduced with D-glucose for 30 minutes and 1 hour showed significantly lower intensity at the concentration of 25µg/ml with 11.35 and 13.17 MFI **(Fig. 5e1,f1)**. In contrast, stabilized Se-NPs reduced with orange for 30 minutes and 1 hour showed lower intensity at the concentration of 15µg/ml with 15.78 and 16.37 MFI **(Fig. 5g1,hl)**. Raju *et al*. performed a similar protocol to assess the LPO levels in zebrafish larvae exposed to H_2O_2 stress, showing similar upregulation in intensity in the stress group, compared to the treatment groups[68].

Estimation of AChE activity

Compared to the control group, zebrafish larvae exposed to $CuSO_4$showed a significant decrease in AChE levels dropping from 1.14 µmol/ml to 0.76µmol/ml. Treatment with 25 µg/ml stabilized Se-NPs reduced with D-glucose for 30 minutes and 1 hour, in $CuSO_4$-exposed zebrafish larvae resulted in a dose-dependent increase in AChE levels, reaching 1.04 and 0.97µmol/ml **(Fig. 6a,b)**, respectively. Conversely, treatment with stabilized Se-NPs reduced with orange peel extract for 30 minutes and 1 hour, only restored

View Article Online
DOI: 10.1039/D4NA00644E

the AChE concentration up to 0.95 and 0.90µmol/ml respectively **(Fig. 6c,d)**.This suggests that stabilized Se-NPs reduced with D-glucose for 30 minutes significantly restored AChE concentration. A study focusing on pentylenetetrazole-induced oxidative stress demonstrated that pentylenetetrazole-exposed mice treated with Se-NPs showed improved AChE levels compared to untreated mice[69].Therefore, stabilized Se-NPs regulated $CuSO_4$-induced neuron damage and protected thecentral nervous system(CNS).

Estimation of Locomotor Activity

To measure the locomotor activity of zebrafish larvaeanddetermine cognitive alterations in the CNS,neurobehavior will be assessed based on the distance travelled by the zebrafish larvae (in meters). Treatment with 25µg/ml of stabilized Se-NPs, reduced with glucose for 30 minutes and 1 hour, improved cognitive behaviour by restoring the covered distance to 93.40 m and 78.79 m in the $CuSO_4$ exposed zebrafish larvae group **(Fig. 6e-n)**. Conversely, treatment with stabilized Se-NPs reduced with orange for 30 minutes and 1 hour at a concentration of 15µg/ml only improved cognitive behaviour by 46.48 m and 44.16 m**(Fig. 6o-x)**. The control group exhibited normal cognitive behaviour with an estimated travelled distance of 102.60 m **(Fig. 6y)**. Following$CuSO_4$exposure, the zebrafish larvae could onlytravel 16.2 m due to stress effects **(Fig. 6z)**, which was restored by approximately 91% with D-glucose reduced nano-Se.It is already established that zinc oxide nanoparticles increase oxidative stress and impair cognitive function by decreasing the expression of Cyclic Adenosine Monophosphateresponse element binding protein (CREB), phosphorylated CREB, and synapsin Iage-dependently[70].At the neuromuscular junction,acetylcholine is primarily released by the motor neuron, acting as a neurotransmitterand regulating fast synaptic currents essential for precise locomotioncontrol[71].Li *et al*. reported that alterations in the central nervous system can be determined by the behavioral changes in animals[72], indicating that stabilized Se-NPs did not affect the central nervous system. D-glucose reduced nano-Se restores the AChE concentration which is directly associated with the formation and release of acetylcholine through synaptic vesicles and controls cognitive properties without altering behavior.

View Article Online
DOI: 10.1039/D4NA00644E

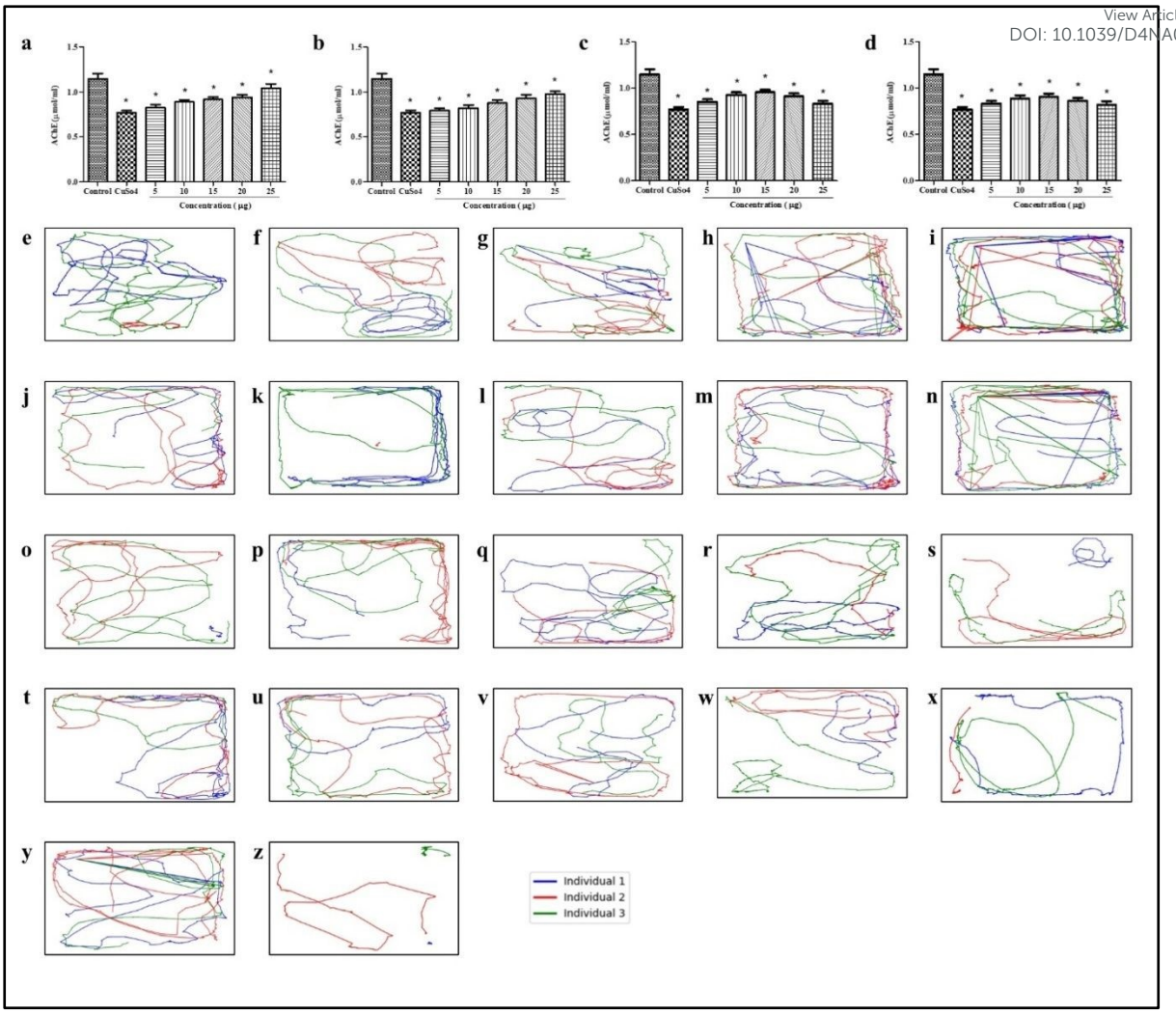

Fig.6 AChE assay and Locomotory Analysis *in vivo* in zebrafish Larvae Treated with Stabilized Se-NPs. AChE assay of (a-b) reduced with D-glucose for 30 minutes and 1 hour, (c-d) reduced with orange peel extract for 30 minutes and1 hour. Locomotor analysisof stabilized Se-NPs reduced with D-glucose for 30 minutes (e) 5 µg/ml, (f) 10 µg/ml, (g) 15 µg/ml, (h) 20 µg/ml, (i) 25 µg/ml; stabilized Se-NPs reduced with D-glucose for 1 hour (j) 5 µg/ml, (k) 10 µg/ml, (l) 15 µg/ml, (m) 20 µg/ml, (n) 25 µg/ml; stabilized Se-NPs reduced with orange peel extract for 30 minutes (o) 5 µg/ml, (p) 10 µg/ml, (q) 15 µg/ml, (r) 20 µg/ml, (s) 25 µg/ml; stabilized Se-NPs reduced with orange peel extract for 1 hour (t) 5 µg/ml, (u) 10 µg/ml, (v) 15 µg/ml, (w) 20 µg/ml, (x) 25 µg/ml; Control (y) Untreated; $CuSO_4$; (z) 20 µM.The data were considered significant ($p < 0.05$) and marked by the symbol "*".

CONCLUSION

In the ETC, mitochondria are a significant source of ROS. Increased ROS production can occur due to impaired mitochondrial function disrupting cellular homeostasis by reducing antioxidant defences and increasing lipid peroxidation. This can lead to various illnesses, including neurodegeneration. Enzymes like SOD, CAT, and GSH act as defense mechanisms to neutralize ROS.One of the essential proteins involved in the production of glutathione is selenoproteins. Deficiency of these selenoproteins also plays a role in decreasing antioxidant enzymes.However, there are several commercial drugs available, such as Coenzyme Q10, N-acetylcysteine, edaravone, Non-Steroidal Anti-Inflammatory Drugs, corticosteroids, memantine, riluzole, selegiline, levodopa, carbidopa, donepezil, etc., that can regulate oxidative stress and enhance neuroprotection. Many researchers have used nanoparticles as carriers to deliver drugs to the target site. These nanoparticles can be considered therapeuticdue to their high precision, less toxic profile, and ability to cross the blood-brain

View Article Online
DOI: 10.1039/D4NA00644E

barrier. Se-NPs have attracted significant interest as a carrierfor various applications, especially in medicine.Generally, they are biocompatible and do not exhibit toxicity compared to other forms of Se.The strong antioxidant properties of Se-NPsmake them effective ROS scavengers that protect cells from oxidative damage.

In our study,mussel-extracted Se was used as a rich source of Se for the synthesis of Se-NPs. Saline extraction yieldeda higher amount compared to the buffer extraction method. FTIR peaks indicated the presence of metal, stabilizer, and reducing agents used. The size of the nanoparticles depended on the reducing agent.D-Glucose efficiently produced nearly spherical nano-Se of 20nm size with potential therapeutic approaches. A comparison between reducing agents showed that a 30-minute reduction with D-glucose produced potent nano-Sein reducing oxidative stress and improving survival rates in $CuSO_4$ stress-induced zebrafish larvae. In the stress group, *in-vivo* treatment with 5-25µg/ml of stabilized Se-NPs reduced with D-glucose showed no toxic effects andsurvival ratesimprovedin a concentration-dependent manner.On the other hand,orange-reducedstabilized Se-NPs were found to be non-toxic only up to 15µg/ml. Moreover,YSE was found to be developed above those concentrations under stress-induced zebrafish larvae *in vivo*. All stabilized Se-NPs showed concentration-dependent DPPH scavenging activity and concentration-independent ABTS scavenging activity.However,the highest scavenging capacity was recorded with nano-Se reduced with D-glucose for 30 minutes.*In-vivo* enzymatic analysis of stabilized Se-NPs reduced with D-glucose for 30 minutes showed a remarkable improvement in antioxidant enzyme levels while decreasing LPO and NO levels in zebrafish larvae. They restored the enzyme levels by producing SOD, CAT, GSH, GST, which may be NRF2 dependent mechanism and significantly reduced the MDA and NO levels ina concentration-dependent manner. The qPCR confirmed that nearly a 2-fold enhancement of antioxidant genes was mitigatingcellular ROS.Live cell imaging also supported the therapeutic property of D-glucose-reduced nano-Se.Additionally, D-glucose reduced nano-Se enhanced AChE levels in a dose-dependent manner. Locomotor analysis confirmed that D-glucose reduced, and stabilized Se-NPs did not disrupt CNS function and improved cognitive functions in stress-induced zebrafish larvae. Thus, treatment with 25µg/ml of D-Glucose reduced nano-Se upregulated the antioxidant gene expression, downregulated LPO and NO levels with an enhancement of AChE production which directly influences the release of acetylcholine from synaptic vesicles and regulates cognitive function without altering the behavior of the larvae. Therefore, D-glucose-reduced Se-NPscould be a potential therapeutic option to reduce oxidative stress and improve cognitive function in oxidative stress-related diseases and disorders.This characteristic makes them safer for therapeutic applications.

Future advancements in combined therapy could involve the integration of Se-NPs with other therapeutic agents to enhance their efficacy. Combining Se-NPs with traditional antioxidants, anti-inflammatory drugs, or targeted delivery systems may synergize their effectsand provide a more effective approach to regulate oxidative stress and stress-related diseases. Further research is necessary on Se-NPs to make significant advancements in the management and treatment of various debilitating conditions, as they have the ability to enhance endogenous antioxidant enzymes and cross the blood-brain barrier.

MATERIALS AND METHODS

Chemicals Used

Sodium Chloride (NaCl) was purchased from Merck (CAS No: 7647-14-5), Tris (hydroxymethyl) aminomethane was purchased from Thermofisher Scientific (CAS No: 77-

View Article Online
DOI: 10.1039/D4NA00644E

86-1). L-Ascorbic acid (CAS No: 50-81-7), Hydrogen peroxide (H_2O_2; CAS: 7722-84-1) and Hydrochloric acid (CAS No: 7647-01-0) were purchased from Sigma-Aldrich. Magnesium chloride (CAS No: 7786-30-3), Calcium chloride (CAS No: 10043-52-4), Sodium phosphate dibasic (CAS No: 7558-79-4), Potassium phosphate monobasic (CAS No: 7778-77-0), Potassium chloride (CAS No: 7447-40-7), NitroBlue Tetrazolium salt (NBT; CAS No: 298-83-9), L-Methionine (CAS No: 63-68-3), Riboflavin (CAS No: 83-88-5), Thiobarbituric acid (TBA; CAS No: 504-17-6), Trichloroacetic acid (TCA; Cc: 76-03-9), Griess reagent (EC: 215-981-2), 5,5'-dithiobis-(2-nitrobenzoic acid) (DTNB; CAS No: 69-78-3), Potassium phosphate dibasic (CAS No: 7758-11-4), 1-chloro 2,4- dinitrobenzene (CAS No: 97-00-7) was purchased from Sigma-Aldrich. BSA was purchased from Sisco Research Laboratories (SRL; CAS No: 9048-46-8). 2,2-Diphenyl-1-Picrylhydrazyl (DPPH; CAS No: 1898-66-4) and 2,2'-azino-bis (3-ethylbenzothiazoline-6-sulfonic acid (ABTS salt; CAS No: 30931-67-0), Dichlorofluorescein diacetate (DCFHDA; CAS No: 2044-85-1), 2,2-Diphenyl-1-Picrylhydrazyl (DPPH; CAS No: 1898-66-4), Potassium Persulfate (CAS No: 7727-21-1), Ethylenediaminetetraacetic acid (EDTA; CAS No: 60-00-4) were purchased from Sisco Research Laboratories (SRL). RDP Trio™ Reagent was collected from HiMedia (SKU: MB566) and AURA 2x One-Step RT-PCR Master Mix was collected from AURA Biotechnologies Pvt Ltd (ABT-18S). Glassware was purchased from Borosil® and 96-well ELISA plates were purchased from ThermoFisher Scientific®.

Extraction of Selenium from Mussels

a) *Collection and Preparation of Mussel*

Mussels (Domain: Eukaryota; Kingdom: Animalia; Phylum: Mollusca; Class: Bivalvia; Order: Mytilida; Family: Mytilidae; Genus: *Perna*; Species: *viridis*) were freshly collected whole from Kasimedu Fishing Harbour, Tondiarpet (N 13° 7' 22.4292", E 80° 17' 36.4272"), Chennai. The mussels were thoroughly cleaned to remove sand and debris. The shells were then opened, and the tissue was carefully scraped and rinsed with distilled water. After removing excess water, the collected tissue was dried overnight. The dried mussel tissue was subsequently stored at 4°C for use in further experiments.

b) *Extraction of Se*

i. Extraction with 0.8% Saline:

A 0.8% saline solution was freshly prepared by dissolving 8 g of sodium chloride (NaCl) in 1000 ml of distilled water. Next, 8.5 g of mussel tissue was weighed and ground with 100 ml of the 0.8% saline solution using a mortar and pestle. The resulting mixture was centrifuged at 5000 rpm for 30 minutes at room temperature (37℃). This centrifugation step was repeated until no pellet was observed. The collected pellet was dried at 60℃ in a hot air oven. Once completely dry, the pellet was ground into a fine powder using a mortar and pestle[73].

ii. Extraction with 50mM Tris-HCl Buffer pH7.4:

A Tris-HCl buffer (pH 7.4) was freshly prepared by dissolving 2.65 g of Tris base and 4.44 g of HCl in 1000 ml of distilled water. Next, 8.5 g of mussel tissue was weighed and ground with 100 ml of the Tris-HCl buffer using a mortar and pestle. Following the method previously described for selenium purification fine Se powder was obtained[73].

Synthesis of Se-NPs

A green synthesis approach was usedto produce Se-NPsby reducing mussel-derived Se, withD-glucose and crude orange peel extract (Schematically represented in flowchart).

View Article Online
DOI: 10.1039/D4NA00644E

Fresh orangeswere purchased from local markets, washed,and their peels were collected. The collected orange peels were blended with 100g in 500ml of water using a mixer, filtered, and stored at 4℃ as needed. 0.2 g of mussel-derived selenium was dissolved in 50 ml of distilled water using a sonicator. In a round bottom flask, 50 ml of the dissolved mussel-derived Se was combined with 15 ml of 0.25 M D-glucose and 15 ml of crude orange peel extract separately. Both reduction processes were carried out at two different intervals, 30 minutes and 1 hour, with and without a stabilizer (5% BSA), using a heating mantle. The resulting mixture was centrifuged at 5000 rpm for 30 minutes at 37℃ (room temperature). The collected pellets were then dried at 60℃ in a hot air oven. Once completely dried, the pellets were ground into a fine powder using a mortar and pestle[47,74]. These synthesized Se-NPs were used for further experimental investigations.

Characterization of Mussel extracted Se and Se-NPs

The Se-NPs underwent a comprehensive analysis utilizing various analytical techniques. Inductively Coupled Plasma Optical Emission Spectroscopy (ICP-OES) was conducted using a PERKIN ELMER OPTIMA 5300 DV ICP-OES to determine trace element concentrations[75].X-ray diffraction (XRD) and crystallography studies were carried outusing a BRUKER D8 ADVANCE POWDER XRD. The measurements were taken over a 2θ range spanning from 10 to 80 degrees[76]. Fourier-transform infrared (FTIR) spectroscopy was used to examine the presence of functional groups. This analysis was performed using a Nicolet Summit FTIR instrument (ThermoFisher Scientific) operating in diffuse reflectance mode. The detectors used were DTGS KBr, and 16 scans were recorded over a wavenumber range from 400 to 4000 cm^{-1}[76]. The resulting spectra were plotted with wavenumber (cm^{-1}) on the X-axis and transmittance (%) on the Y-axis using OriginPro 8.5 Software. Scanning Electron Microscope (SEM) analysis was conducted using a Hitachi Model: S-3400N to elucidate the surface morphology of the Se-NPs. The SEM was operated at 15 kV in high vacuum (HV) mode with semiconductor secondary electron (SE) detection. The acquired images were further analyzed for size distribution using ImageJ software[76]. TEM and SAED (FEI Tecnai G2 20 S-TWIN TEM) was operated at 200 kV. Particle size analysis and Zeta potential were done using nanoPartica SZ-100V2 (Horiba)[76].

In Vitro Antioxidant Studies

To evaluate the *in vitro* antioxidant potential of stabilized Se-NPs, DPPH and ABTS assays were conducted following methods outlined in previous studies[77,78].Stock solutionscontaining 50 µM ascorbic acid and 1 mg/ml of Se-NPswere prepared from which working solutions of 5, 10, 15, 20 and 25 µg/ml were derived. These concentrations werefixed based on previously reported studies[79]and were consistently utilized throughout the study.Three individual experiments were performed.

a) DPPH Assay

In this method, a DPPH solution of 300 µM was mixed with 50 µM ascorbic acid and various concentrations of stabilized Se-NPs (5, 10, 15, 20, and 25 µg/ml) in a 96-well ELISA plate. The plates were then incubated in darkness for 30 minutes. After the incubation period, the absorbance of the samples was measured at 517 nm using a ThermoFisher Scientific® microplate reader.

b) ABTS Assay

The reaction mixture of 7 mM ABTS salt prepared with 2.45 mM potassium persulfate (1:1) was incubated for 24 hours in the dark at room temperature. To achieve an

absorbance of 0.7±2 at 734 nm, 20X PBS was used to dilute the ABTS solution, 50 µM ascorbic acid was used as a positive control along with stabilized Se-NPs (5, 10, 15, 20 and 25 µg/ml). These were added to a 96-well ELISA plate along with the ABTS solution. The plate was then incubated at room temperature in the dark for an hour. The samples were measured at 734 nm using a ThermoFisher Scientific® microplate reader.

In Vivo Developmental Toxicity Studies

a) Zebrafish Maintenance and Embryo Collection

Adult male and female zebrafish were obtained from Tarun Fish Farm in Manimangalam (latitude N 12° 55' 1" and longitude E 80° 2' 29"), Chennai. Based on Institutional Ethical Committee Guidelines (SU/CLAR/RD/001/2023), adult zebrafish were maintained in a 19 L glass tank at 28.5℃ with a 14/10 hour light/dark cycle. The fish were fed live *Artemia salina* (brine shrimp) threetimes a day. Breeding was initiated after 20 days of acclimatization in lab conditions. Two separatebreeding groups were placed in a spawning tank with a ratio of 1:1 (male:female). To prevent the female fish from swallowing the eggs, a mesh was placed at the bottom of the spawning tank. Embryos were collected from the breeding unit 30 minutes after the onset of light. The embryos were rinsed with freshly prepared E3 medium[80] and kept at 26 ± 1°C (OECD, 2013) until the experiments were conducted.

b) *In Vivo Developmental Toxicity Test*

Zebrafish embryos (4 hours post fertilization; hpf) were transferred to a 12-well plate (n=10 embryos per well). The control group embryos were left untreated. The embryos were exposed to $CuSO_4$ (20 µM; stress group) and $CuSO_4$exposed group treated with 5 different concentrations of stabilized Se-NPs(5-25µg/ml) every 24 hours until 96 hours. These concentrations were fixed based on previously reported studies[51,81,82]and were consistently utilized throughout the study.The experiment was conducted in triplicate. The development of the zebrafish embryos was observed under a microscope at 4X magnification[83,84].

In Vivo Antioxidant Studies

For enzymatic assays, the $CuSO_4$-exposed larvaetreated with stabilized Se-NPs(5-25 µg/ml) were homogenized (n = 20, all experiments were conducted in triplicate) in a solution containing 100 mM Tris HCl buffer (pH 7.8 at 4℃) with 150 mM potassium chloride and 1 mM EDTA, at 96 hpf. The homogenized sample was centrifuged at 10000 rpm for 15 minutes and the supernatant was used for further enzymatic analysis[85]. The Bradfordmethod was used for protein estimation[86].

a) Superoxide Dismutase (SOD) Assay

A reaction mixture consisting of 50mM phosphate buffer (pH 7.8), 100µM EDTA, 750 µM NBT, 130 mM methionine, and 20µM riboflavin was prepared and added to the 50 µl larval homogenate. The mixture was incubated under light for 20 minutes and absorbance was measured at 560 nm[84].

b) Catalase (CAT) Assay

The catalase assay was done based on a previously reported study[87]. To determine catalase activity, 100 µl of buffered H_2O_2 was added to 50µl of the sample. The absorbance was noted at 240nm for 2 minutes with an interval of 15 seconds using spectrophotometry.

View Article Online
DOI: 10.1039/D4NA00644E

c) Lipid Peroxidation (LPO) Assay

MDA levels were determined using the thiobarbituric acid method[87]. To a 100 µl sample, 0.1 ml of 5% trichloroacetic acid was added and incubated for 15 minutes on ice. Then, 0.2 ml of 0.67% thiobarbituric acid was added and incubated for 30 minutes at 100℃ in a water bath. The sample was cooled immediately on ice for 20 minutes and then centrifuged at 2000 rpm for 10 minutes at 4℃. The absorbance was recorded at 535nm [88].

d) Nitric Oxide (NO) Assay

The Griess method was employed to determine NO levels, with slight modifications[89]. 100µl Griess reagent was added to the 100µl homogenized larvae sample. The samples were incubated for 25 minutes at room temperature. The absorbance was noted at 540 nm.

e) *Reduced Glutathione (GSH) and Glutathione S-Transferase(GST) Assay*

GSH and GST assays were performed as described by Issac *et al*.[84], with minor modifications. To estimate GSH levels, a 100 µl larvae sample was mixed with 50 µl of 20 mM DTNB and 150µl of 100 mM potassium phosphate buffer with a pH of 7.4. The absorbance was measured at 412 nm. To determine GST levels, a 100 µl reaction mixture containing 10 µM GSH and 60 µM 1-chloro 2,4-dinitrobenzene was prepared and added to 50 µl of the larvae sample, and the absorbance was recorded at 340 nm.

Antioxidant Gene Expression by Real-Time Polymerase Chain Reaction (RT-PCR)

RNA was extracted from the experimental homogenized zebrafish larvae using RDP Trio™ Reagent. The primers for antioxidant enzymes and housekeeping genes were designed using NCBI's Primer-BLAST **(Table 1)**. Expression of the genes was analyzed using AURA 2x One-Step RT-PCR Master Mix. The reverse transcription process starts with a singlecycle at a temperature ranging between 44-50℃lasting for 15 minutes, followed by enzyme activation, at 95℃ for 3 minutes. The denaturation step (repeated for 40 cycles) was at 95℃ for 10 seconds. Annealing was done at 60℃for 45 seconds, and the extension process was performedat 72℃ for 15 seconds. The fold changewas calculated using the $2^{-\Delta\Delta ct}$ method[77].

Estimation of Acetylcholinesterase (AChE)

The larvae were analyzed for cognitive impairments after exposure to $CuSO_4$ and treatment with stabilized Se-NPs. The homogenized larvae were centrifuged at 5000 rpm for 15 minutes. The supernatant was mixed with thereaction mixture containing 3.3 mM DTNB and incubated for 20 minutes. Theabsorbance was recorded at 412 nm in 1minuteintervals following the acetylcholine iodideaddition[72,77].

Cognitive Behavior Analysis

The locomotor abnormalities of the zebrafish larvae were evaluated by analyzing the swimming behavior pattern[90]. At the end of the exposure period (7 dpf) each exposure group (n = 3 larvae/well;experiments were conducted in triplicate) was placed in a white chambered ice tray (2.5 × 3.5 cm) containing 2 ml of E3 medium prepared without methylene blue, for 10 minutes of acclimatization. The locomotion of larvae was recorded at the beginning of the light cycle under noise-free conditions by a commercial smartphone camera after acclimatization. The video was recorded for 60 seconds at 60 frames per second and locomotion was plotted using UMA Tracker software[91].

Estimation of ROS Levels in Zebrafish Larvae

All groups including the control, stress group and stabilised Se-NPs treated group larvae were anaesthetized (n = 6 per group) using tricaine. The larvae were stained with DCFDA (20 µg/ml) dye and incubated for 1 hour in the dark at room temperature. After incubation, the stained larvae were observed pictographically under a fluorescentmicroscope (CKX53 Microscope, Japan) and analyzed using ImageJ software[92].

Estimation of LPO Levels in Zebrafish Larvae

All groups including the control, stress group and stabilised Se-NPs treated group larvae were anaesthetized (n = 6 per group) using tricaine. The larvae were stained with DPPP (25 µg/ml) dye and incubated for 30 minutes at room temperature. After incubation, the stained larvae were observed pictographically under a fluorescentmicroscope (CKX53 Microscope, Japan) and analyzed using ImageJ software[92].

Statistical Analysis

All experiments in this study were conducted in triplicate and are presented as mean ± standard deviation (SD). The data was analyzed using one-way analysis of variance (ANOVA) and Dunnett's Multiple Comparison Test in GraphPad Prism 5.0 (GraphPad Software, Inc., San Diego, CA)[93]. Significant results were denoted by the symbol "*" and were considered significant with $p < 0.05$.

DECLARATIONS

ETHICS APPROVAL AND CONSENT TO PARTICIPATE

All experiments were conducted in accordance with the ethical guidelines for the care and utilization of animals, as approved by the Institutional Ethical Committee under protocol number SU/CLAR/RD/001/2023.

LIVE SUBJECT STATEMENT

All experiments were performed in compliance with OECD guidelines. All animal procedures were performed in accordance with the Guidelines for Care and Use of Laboratory Animals of Saveetha Institute of Medical and Technical Sciences, Saveetha University and approved by the Institutional Animal Ethics Committee of Saveetha Medical College. No human subjects were used throughout the study.

CONSENT FOR PUBLICATION

Not applicable

AVAILABILITY OF DATA AND MATERIALS

All data generated or analyzed during this study are included in this published article. Data for this article, including qPCR primers are available at NCBI (NCBI: NM_131294.1; NCBI: XM_021470442.1; NCBI: XM_005169592.4; NCBI: NM_001030070.2;NCBI: NM_131031.2) at https://www.ncbi.nlm.nih.gov/;SOD: https://www.ncbi.nlm.nih.gov/nuccore/NM_131294.1;CAT: https://www.ncbi.nlm.nih.gov/nuccore/XM_021470442.1;GSR:

View Article Online
DOI: 10.1039/D4NA00644E

https://www.ncbi.nlm.nih.gov/nuccore/XM_005169592.4;GPx: https://www.ncbi.nlm.nih.gov/nuccore/NM_001030070.2;Beta actin: https://www.ncbi.nlm.nih.gov/nuccore/NM_131031.2

SUPPLEMENTARY DATA

There is a supplementary file with figures, tables and raw data sheet along with the main manuscript.

COMPETING INTERESTS

The authors declare that they have no competing interests

FUNDING

This research did not receive any specific grant from funding agencies in the public, commercial, or not-for-profit sectors.

AUTHORS' CONTRIBUTIONS

SU is responsible for conducting experiments, result analysis, and figures and IP is responsible for conceptualization, result validation. Both the authors are writing the original draft and verified the final manuscript.

ACKNOWLEDGEMENT

We express our gratitude to the Saveetha School of Engineering, Saveetha Institute of Medical and Technical Sciences, Saveetha University, for providing the necessary infrastructure to carry out this work successfully.

FIGURE LEGENDS

Fig. 1 Synthesis and Characterization of Se extracted from mussel and Se-NPs: ICP-OES (a) Saline extracted Se; (b) Buffer extracted Se; XRD analysis (c) Saline extracted Se; (d) Buffer extracted Se; SEM (e-f) stabilized Se-NPs reduced for 30 minutes and 1hour with D-glucose; (g-h) stabilized Se-NPs reduced for 30 minutes and 1hour with orange; TEM and SAED (i-j) stabilized Se-NPs reduced for 30 minutes with D-Glucose; (k-l) stabilized Se-NPs reduced for 30 minutes with orange. Yield (m) Percentage of Se yield. FTIR (n) stabilized Se-NPs reduced for 30 minutes and 1 hour with D-glucose; (o) stabilized Se-NPs reduced for 30 minutes and 1 hour with orange peel extract.

Fig.2 *In Vivo* Developmental Toxicity Analysis in zebrafish embryos and larvae representing, Control group; Stress group ($CuSO_4$-induced stress); and Stabilized Se-NPs (5-25 µg/ml) treatment group. (a-b) stabilized Se-NPs reduced with D-glucose for 30 minutes and 1 hour, (c-d) stabilized Se-NPs reduced with orange peel extract for 30 minutes and 1hour. Survival rate (a1-b1) stabilized Se-NPs reduced with D-glucose for 30 minutes and 1 hour, (c1-d1) stabilized Se-NPs reduced with orange peel extract for 30 minutes and 1hour.The data were considered significant ($p < 0.05$) and marked by the symbol "*".

Fig. 3 *In Vitro* Antioxidant Activity: DPPH assay of (a-b) stabilized Se-NPs reduced with D-glucose for 30 minutes and 1 hour, (c-d) stabilized Se-NPs reduced with orange peel extract for 30 minutes and 1hour. ABTS assay of (e-f) stabilized Se-NPs reduced with D-glucose for 30 minutes and 1 hour, (g-h) stabilized Se-NPs reduced with orange peel extract for 30 minutes and 1hour.The data were considered significant ($p < 0.05$) and marked by the symbol "*".

View Article Online
DOI: 10.1039/D4NA00644E

Fig. 4 *In Vivo* Antioxidant Activity of stabilized Se-NPs: SOD assay (a-b) reduced with D-glucose for 30 minutes and 1 hour, CAT assay (c-d) reduced with D-glucose for 30 minutes and 1 hour. LPO assay (e-f) reduced with D-glucose for 30 minutes and 1 hour. NO assay (g-h) reduced with D-glucose for 30 minutes and 1 hour. GSH assay (i-j) reduced with D-glucose for 30 minutes and 1 hour. GST assay (k-l) reduced with D-glucose for 30 minutes and 1 hour. RT-PCR (m) reduced with D-glucose for 30 minutes (25 µg/ml). The data were considered significant ($p < 0.05$) and marked by the symbol "*".

Fig. 5 Live Cell Imaging *In Vivo* in the Zebrafish Larvae Model at 96 HPF: DCFDA staining (a&a1) stabilized Se-NPs reduced with D-glucose for 30 minutes & MFI; (b & b1) stabilized Se-NPs reduced with D-glucose for 1 hour &MFI; (c&c1) stabilized Se-NPs reduced with orange peel extract for 30 minutes &MFI; (d & d1) stabilized Se-NPs reduced with orange peel extract for 1 hour & MFI. DPPP staining (e & e1) stabilized Se-NPs reduced with D-glucose for 30 minutes &MFI; (f & f1) stabilized Se-NPs reduced with D-glucose for 1 hour &MFI. (g & g1) stabilized Se-NPs reduced with orange peel extract for 30 minutes & MFI; (h & h1) stabilized Se-NPs reduced with orange peel extract for 1 hour & MFI. The data were considered significant ($p < 0.05$) and marked by the symbol "*".

Fig. 6 AChE assay and Locomotory Analysis *in vivo* in zebrafish Larvae Treated with Stabilized Se-NPs.AChE assay of (a-b) reduced with D-glucose for 30 minutes and 1 hour, (c-d) reduced with orange peel extract for 30 minutes and1 hour. Locomotor analysis of stabilized Se-NPs reduced with D-glucose for 30 minutes (e) 5 µg/ml, (f) 10 µg/ml, (g) 15 µg/ml, (h) 20 µg/ml, (i) 25 µg/ml; stabilized Se-NPs reduced with D-glucose for 1 hour (j) 5 µg/ml, (k) 10 µg/ml, (l) 15 µg/ml, (m) 20 µg/ml, (n) 25 µg/ml; stabilized Se-NPs reduced with orange peel extract for 30 minutes (o) 5 µg/ml, (p) 10 µg/ml, (q) 15 µg/ml, (r) 20 µg/ml, (s) 25 µg/ml; stabilized Se-NPs reduced with orange peel extract for 1 hour (t) 5 µg/ml, (u) 10 µg/ml, (v) 15 µg/ml, (w) 20 µg/ml, (x) 25 µg/ml; Control (y) Untreated; $CuSO_4$; (z) 20 µM. The data were considered significant ($p < 0.05$) and marked by the symbol "*".

TABLE LEGEND

Table 1: Primer sequences used in RT-PCR

View Article Online
DOI: 10.1039/D4NA00644E

779 **Table 1: Primer sequences used in RT-PCR**

Gene	Forward Primer(5' to 3')	Reverse Primer (5' to 3')	Reference
SOD	GGTCCGCACTTCAACCCTCA	TACCCAGGTCTCCGACGTGT	NCBI: NM_131294.1
CAT	AACTGTGGAAGGAGGGTCGC	CGCTCTCGGTCAAAATGGGC	NCBI: XM_021470442.1
GSR	GATGGGCACCATAGCTAACCC	CATGAGCAGGAAGCAACACCC	NCBI: XM_005169592.4
GPx	AACTACACTCAGCTTGCGGC	TCCGCTTCACTTCCAGGCTC	NCBI: NM_001030070.2
β-actin	AAGCTGTGACCCACCTCACG	GGCTTTGCACATACCGGAGC	NCBI: NM_131031.2

780

781 EXTRACTION METHOD FLOWCHART

View Article Online
DOI: 10.1039/D4NA00644E

782

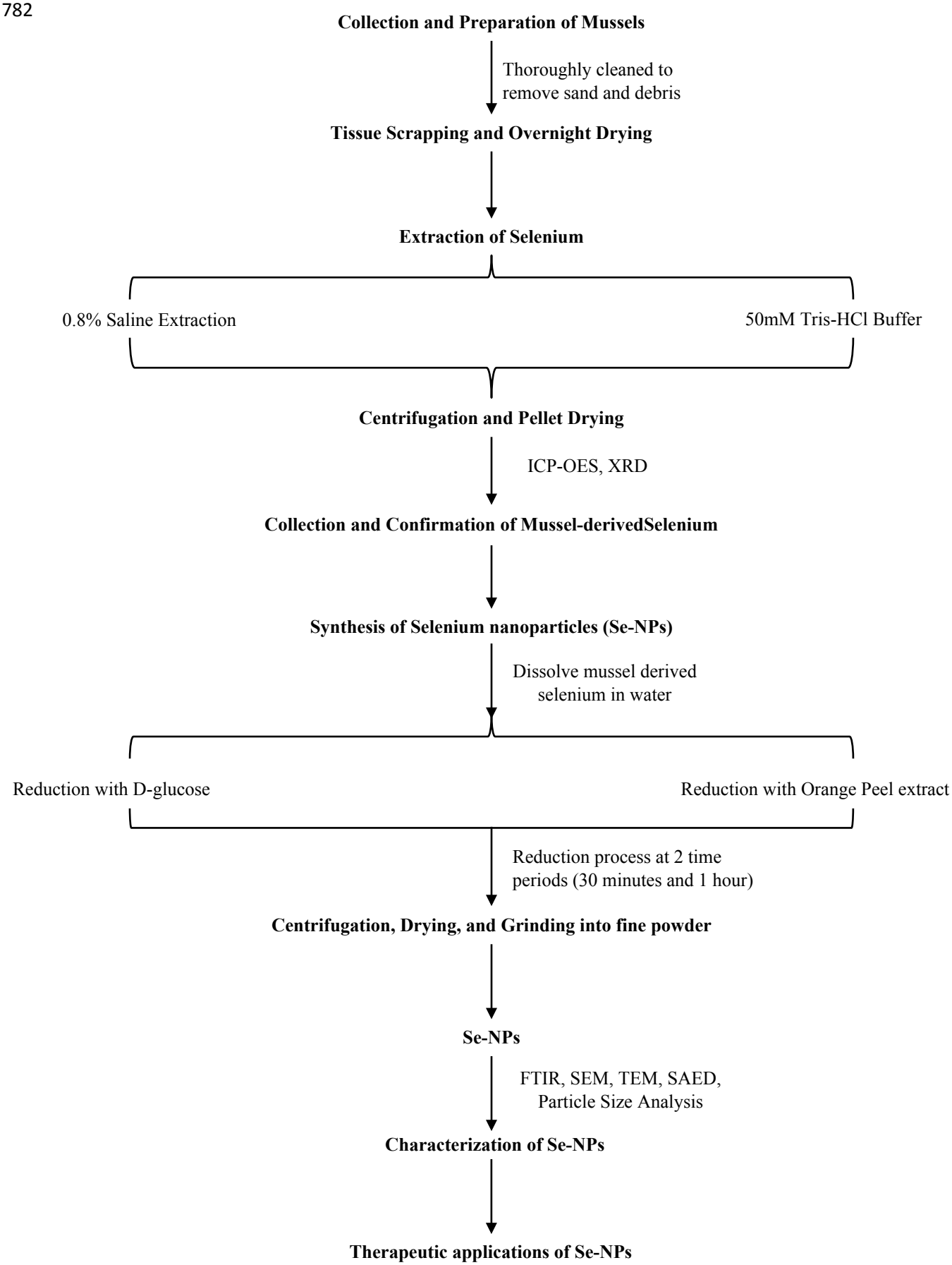

View Article Online
DOI: 10.1039/D4NA00644E

REFERENCES

1 L. D. Osellame, T. S. Blacker and M. R. Duchen, *Best Pract. Res. Clin. Endocrinol. Metab.*, 2012, **26**, 711–723.

2 L.-D. Popov, *Cell. Signal.*, 2023, **109**, 110794.

3 F. A. Bustamante-Barrientos, N. Luque-Campos, M. J. Araya, E. Lara-Barba, J. de Solminihac, C. Pradenas, L. Molina, Y. Herrera-Luna, Y. Utreras-Mendoza, R. Elizondo-Vega, A. M. Vega-Letter and P. Luz-Crawford, *J. Transl. Med.*, 2023, **21**, 613.

4 D. M. Niyazov, S. G. Kahler and R. E. Frye, *Mol. Syndromol.*, 2016, **7**, 122–137.

5 R. N. L. Lamptey, B. Chaulagain, R. Trivedi, A. Gothwal, B. Layek and J. Singh, *Int. J. Mol. Sci.*, 2022, **23**, 1851.

6 W. Chen, H. Zhao and Y. Li, *Signal Transduct. Target. Ther.*, 2023, **8**, 333.

7 T. Vezza, P. Díaz-Pozo, F. Canet, A. M. de Marañón, Z. Abad-Jiménez, C. García-Gargallo, I. Roldan, E. Solá, C. Bañuls, S. López-Domènech, M. Rocha and V. M. Víctor, *World J. Mens. Health*, 2022, **40**, 399.

8 S. K. Bardaweel, M. Gul, M. Alzweiri, A. Ishaqat, H. A. ALSalamat and R. M. Bashatwah, *Eurasian J. Med.*, 2018, **50**, 193–201.

9 G. Pizzino, N. Irrera, M. Cucinotta, G. Pallio, F. Mannino, V. Arcoraci, F. Squadrito, D. Altavilla and A. Bitto, *Oxid. Med. Cell. Longev.*, 2017, **2017**, 1–13.

10 Tsatsakis, Docea, Calina, Tsarouhas, Zamfira, Mitrut, Sharifi-Rad, Kovatsi, Siokas, Dardiotis, Drakoulis, Lazopoulos, Tsitsimpikou, Mitsias and Neagu, *J. Clin. Med.*, 2019, **8**, 1295.

11 K. H. Al-Gubory, C. Garrel, P. Faure and N. Sugino, *Reprod. Biomed. Online*, 2012, **25**, 551–560.

12 M. Sharifi-Rad, N. V. Anil Kumar, P. Zucca, E. M. Varoni, L. Dini, E. Panzarini, J. Rajkovic, P. V. Tsouh Fokou, E. Azzini, I. Peluso, A. Prakash Mishra, M. Nigam, Y. El Rayess, M. El Beyrouthy, L. Polito, M. Iriti, N. Martins, M. Martorell, A. O. Docea, W. N. Setzer, D. Calina, W. C. Cho and J. Sharifi-Rad, *Front. Physiol.*, , DOI:10.3389/fphys.2020.00694.

13 S. E. Laouini, A. Bouafia, A. V. Soldatov, H. Algarni, M. L. Tedjani, G. A. M. Ali and A. Barhoum, *Membranes (Basel).*, 2021, **11**, 468.

14 C. E. Probst, P. Zrazhevskiy, V. Bagalkot and X. Gao, *Adv. Drug Deliv. Rev.*, 2013, **65**, 703–718.

15 Z. S. Bailey, E. Nilson, J. A. Bates, A. Oyalowo, K. S. Hockey, V. S. S. S. Sajja, C. Thorpe, H. Rogers, B. Dunn, A. S. Frey, M. J. Billings, C. A. Sholar, A. Hermundstad, C. Kumar, P. J. VandeVord and B. A. Rzigalinski, *J. Neurotrauma*, 2020, **37**, 1452–1462.

16 F. Karimi, N. Rezaei-savadkouhi, M. Uçar, A. Aygun, R. N. Elhouda Tiri, I. Meydan, E. Aghapour, H. Seckin, D. Berikten, T. Gur and F. Sen, *Food Chem. Toxicol.*, 2022, **169**, 113406.

17 R. Gil-Gonzalo, D. A. Durante-Salmerón, S. Pouri, E. Doncel-Pérez, A. R. Alcántara, I. Aranaz and N. Acosta, *Pharmaceutics*, , DOI:10.3390/pharmaceutics16081036.

18 K. R. Trabbic, K. A. Kleski and J. J. Barchi, *ACS Bio Med Chem Au*, 2021, **1**, 31–43.

19 A. M. El Shafey, *Green Process. Synth.*, 2020, **9**, 304–339.

20 M. Kieliszek, *Molecules*, 2019, **24**, 1298.

21 L. Di Renzo, P. Gualtieri, G. Frank and A. De Lorenzo, *Nutrients*, 2023, **15**, 2253.

22 F. Barzegarparay, H. Najafzadehvarzi, R. Pourbagher, H. Parsian, S. M. Ghoreishi and S. Mortazavi-Derazkola, *Biomass Convers. Biorefinery*, 2024, **14**, 25369–25378.

23 F. Chen, X. H. Zhang, X. D. Hu, P. D. Liu and H. Q. Zhang, *Artif. Cells, Nanomedicine, Biotechnol.*, 2018, **46**, 937–948.

24 N. Bisht, P. Phalswal and P. K. Khanna, *Mater. Adv.*, 2022, **3**, 1415–1431.

25 J. T. Tendenedzai, E. M. N. Chirwa and H. G. Brink, *Sci. Rep.*, 2023, **13**, 20379.

26 G. Rusip, S. Ilyas, I. N. E. Lister, C. N. Ginting and I. Mukti, *F1000Research*, 2022, **10**, 1061.

27 O. A. Mahdy, S. Z. Abdel-Maogood, M. Abdelsalam and M. A. Salem, *BMC Vet. Res.*, 2024, **20**, 60.

28 N. Liu, L. Tong, K. Li, Q. Dong and J. Jing, *Molecules*, 2024, **29**, 2414.

29 S. Salaramoli, H. Amiri, H. R. Joshaghani, M. Hosseini and S. I. Hashemy, *Metab. Brain Dis.*, 2023, **38**, 2055–2064.

30 N. Zakeri, M. R. Kelishadi, O. Asbaghi, F. Naeini, M. Afsharfar, E. Mirzadeh and S. kasra Naserizadeh, *PharmaNutrition*, 2021, **17**, 100263.

31 O. M. El-Borady, M. S. Othman, H. H. Atallah and A. E. Abdel Moneim, *Heliyon*, 2020, **6**, e04045.

32 M. Iranifam, M. Fathinia, T. Sadeghi Rad, Y. Hanifehpour, A. R. Khataee and S. W. Joo, *Talanta*, 2013, **107**, 263–269.

33 H. Amani, R. Habibey, F. Shokri, S. J. Hajmiresmail, O. Akhavan, A. Mashaghi and H. Pazoki-Toroudi, *Sci. Rep.*, 2019, **9**, 6044.

34 T. Yin, L. Yang, Y. Liu, X. Zhou, J. Sun and J. Liu, *Acta Biomater.*, 2015, **25**, 172–183.

35 L. Qiao, Y. Chen, X. Song, X. Dou and C. Xu, *Int. J. Nanomedicine*, 2022, **Volume 17**, 4807–4827.

36 Z. Li, H. Liang, Y. Wang, G. Zheng and L. Yang, *ACS Appl. Nano Mater.*, 2024, **7**, 20411–20424.

37 M. Zhu, Y. Zhang, C. Zhang, L. Chen and Y. Kuang, *J. Biomater. Appl.*, 2023, **38**, 109–121.

38 H. Zhao, J. Song, T. Wang and X. Fan, *Nanomedicine Nanotechnology, Biol. Med.*, 2024, **59**, 102755.

View Article Online
DOI: 10.1039/D4NA00644E

39 B. Bálint, K. Balogh, M. Mézes and B. Szabó, *Eur. J. Soil Biol.*, 2021, **107**, 103361.

40 S. Shoeibi, P. Mozdziak and A. Golkar-Narenji, *Top. Curr. Chem.*, 2017, **375**, 88.

41 T. M. Sakr, M. Korany and K. V. Katti, *J. Drug Deliv. Sci. Technol.*, 2018, **46**, 223–233.

42 S. Hariharan and S. Dharmaraj, *Inflammopharmacology*, 2020, **28**, 667–695.

43 A. Tyburska, K. Jankowski, A. Ramsza, E. Reszke, M. Strzelec and A. Andrzejczuk, *J. Anal. At. Spectrom.*, 2010, **25**, 210–214.

44 R. Hassanien, A. A. I. Abed-Elmageed and D. Z. Husein, *ChemistrySelect*, 2019, **4**, 9018–9026.

45 A. M. El Badawy, K. G. Scheckel, M. Suidan and T. Tolaymat, *Sci. Total Environ.*, 2012, **429**, 325–331.

46 T. Nie, H. Wu, K.-H. Wong and T. Chen, *J. Mater. Chem. B*, 2016, **4**, 2351–2358.

47 S. S. Salem, M. S. E. M. Badawy, A. A. Al-Askar, A. A. Arishi, F. M. Elkady and A. H. Hashem, *Life*, 2022, **12**, 893.

48 C. Van der Horst, B. Silwana, E. Iwuoha and V. Somerset, *Anal. Lett.*, 2015, **48**, 1311–1332.

49 A. Bhattacharyya, R. Prasad, A. A. Buhroo, P. Duraisamy, I. Yousuf, M. Umadevi, M. R. Bindhu, M. Govindarajan and A. L. Khanday, *J. Nanosci.*, 2016, **2016**, 1–7.

50 V. Alagesan and S. Venugopal, *Bionanoscience*, 2019, **9**, 105–116.

51 K. Kalishwaralal, S. Jeyabharathi, K. Sundar and A. Muthukumaran, *Artif. Cells, Nanomedicine, Biotechnol.*, 2016, **44**, 471–477.

52 S.-H. Cha, J.-H. Lee, E.-A. Kim, C. H. Shin, H.-S. Jun and Y.-J. Jeon, *RSC Adv.*, 2017, **7**, 46164–46170.

53 J. Vyas and S. Rana, *Int. J. Curr. Pharm. Res.*, 2017, **9**, 147.

54 X. Zhai, C. Zhang, G. Zhao, S. Stoll, F. Ren and X. Leng, *J. Nanobiotechnology*, 2017, **15**, 4.

55 S. Naz, R. Hussain, Z. Guangbin, A. M. M. Chatha, Z. U. Rehman, S. Jahan, M. Liaquat and A. Khan, *Front. Vet. Sci.*, , DOI:10.3389/fvets.2023.1142042.

56 M. A. Khan, D. Singh, A. Arif, K. K. Sodhi, D. K. Singh, S. N. Islam, A. Ahmad, K. Akhtar and H. R. Siddique, *Life Sci.*, 2022, **305**, 120792.

57 M. de los Á. Sariñana-Navarrete, Á. Morelos-Moreno, E. Sánchez, G. Cadenas-Pliego, A. Benavides-Mendoza and P. Preciado-Rangel, *Agronomy*, 2023, **13**, 652.

58 M. Lesnichaya, E. Karpova and B. Sukhov, *Colloids Surfaces B Biointerfaces*, 2021, **197**, 111381.

59 S. S. Anuse, V. SUMATHI, C. UMA, D. SANGEETHA, P. SIVAGURUNATHAN and D. J. M. KUMAR, *UTTAR PRADESH J. Zool.*, 2022, 115–120.

60 O. M. El-Borady, M. S. Othman, H. H. Atallah and A. E. Abdel Moneim, *Heliyon*, 2020, **6**, e04045.

61 P. Horky, B. Ruttkay-Nedecky, M. Kremplova, O. Krystofova, R. Kensova, D. Hynek, P. Babula, O. Zitka, L. Zeman, V. Adam and R. Kizek, *Int. J. Electrochem. Sci.*, 2013, **8**, 6162–6179.

62 J. Mu, L. Lei, Y. Zheng, J. Liu, J. Li, D. Li, G. Wang and Y. Liu, *Antioxidants*, 2023, **12**, 796.

63 G. Barchielli, A. Capperucci and D. Tanini, *Antioxidants*, 2022, **11**, 251.

64 X. Wang, C. X. Hai, X. Liang, S. X. Yu, W. Zhang and Y. L. Li, *J. Ethnopharmacol.*, 2010, **127**, 424–432.

65 J. Fang, H. Yin, Z. Yang, M. Tan, F. Wang, K. Chen, Z. Zuo, G. Shu, H. Cui, P. Ouyang, H. Guo, Z. Chen, C. Huang, Y. Geng and W. Liu, *Ecotoxicol. Environ. Saf.*, 2021, **208**, 111610.

66 M. Hammad, M. Raftari, R. Cesário, R. Salma, P. Godoy, S. N. Emami and S. Haghdoost, *Antioxidants*, 2023, **12**, 1371.

67 N. Handa, S. K. Kohli, A. Sharma, A. K. Thukral, R. Bhardwaj, E. F. Abd_Allah, A. A. Alqarawi and P. Ahmad, *Environ. Exp. Bot.*, 2019, **161**, 180–192.

68 S. V. Raju, A. Mukherjee, P. Sarkar, P. K. Issac, C. Lite, B. A. Paray, M. K. Al-Sadoon, A. R. Al-Mfarij and J. Arockiaraj, *Fish Physiol. Biochem.*, 2021, **47**, 1073–1085.

69 K. M. Mohamed, M. S. Abdelfattah, M. El-khadragy, W. A. Al-Megrin, A. Fehaid, R. B. Kassab and A. E. Abdel Moneim, *Green Process. Synth.*, , DOI:10.1515/gps-2023-0010.

70 L. Tian, B. Lin, L. Wu, K. Li, H. Liu, J. Yan, X. Liu and Z. Xi, *Sci. Rep.*, 2015, **5**, 16117.

71 M. Rima, Y. Lattouf, M. Abi Younes, E. Bullier, P. Legendre, J.-M. Mangin and E. Hong, *Sci. Rep.*, 2020, **10**, 15338.

72 F. Li, J. Lin, X. Liu, W. Li, Y. Ding, Y. Zhang, S. Zhou, N. Guo and Q. Li, *Ann. Transl. Med.*, 2018, **6**, 173–173.

73 U. Kristan, P. Planinšek, L. Benedik, I. Falnoga and V. Stibilj, *Chemosphere*, 2015, **119**, 231–241.

74 T. Nie, H. Wu, K. H. Wong and T. Chen, *J. Mater. Chem. B*, 2016, **4**, 2351–2358.

75 J. Machat, V. Otruba and V. Kanicky, *J. Anal. At. Spectrom.*, 2002, **17**, 1096–1102.

76 C. Ramamurthy, K. S. Sampath, P. Arunkumar, M. S. Kumar, V. Sujatha, K. Premkumar and C. Thirunavukkarasu, *Bioprocess Biosyst. Eng.*, 2013, **36**, 1131–1139.

77 P. K. Issac and K. Velumani, *Bionanoscience*, , DOI:10.1007/s12668-024-01430-z.

78 N. S. Dumore and M. Mukhopadhyay, *J. Mol. Struct.*, 2020, **1205**, 127637.

79 A. J. Kora, *IET nanobiotechnology*, 2018, **12**, 658–662.

80 S. Y. Williams and B. J. Renquist, *J. Vis. Exp.*, , DOI:10.3791/53297.

81 F. Gao, Z. Yuan, L. Zhang, Y. Peng, K. Qian and M. Zheng, *Nanomaterials*, 2023, **13**,

2629.

82 K. Kalishwaralal, S. Jeyabharathi, K. Sundar and A. Muthukumaran, *Artif. Cells, Nanomedicine, Biotechnol.*, 2015, 1–7.

83 Y. Wang, J. Tian, F. Shi, X. Li, Z. Hu and J. Chu, *Microbiol. Immunol.*, 2021, **65**, 410–421.

84 P. K. Issac, A. Guru, M. Velayutham, R. Pachaiappan, M. V. Arasu, N. A. Al-Dhabi, K. C. Choi, R. Harikrishnan and J. Arockiaraj, *Life Sci.*, 2021, **283**, 119864.

85 C. Lite, A. Guru, M. Juliet and J. Arockiaraj, *Environ. Toxicol.*, 2022, **37**, 1988–2004.

86 M. M. Bradford, *Anal. Biochem.*, 1976, **72**, 248–54.

87 M. Velayutham, B. Ojha, P. K. Issac, C. Lite, A. Guru, M. Pasupuleti, M. V. Arasu, N. A. Al-Dhabi and J. Arockiaraj, *Cell Biol. Int.*, 2021, **45**, 2331–2346.

88 P. K. Issac, J. J. Santhi, V. A. Janarthanam and K. Velumani, *Bionanoscience*, , DOI:10.1007/s12668-024-01383-3.

89 K. Schulz, S. Kerber and M. Kelm, *Nitric Oxide*, 1999, **3**, 225–234.

90 M. Krishnan and S. C. Kang, *Neurotoxicol. Teratol.*, 2019, **74**, 106811.

91 O. Yamanaka and R. Takeuchi, *J. Exp. Biol.*, , DOI:10.1242/jeb.182469.

92 G. Sudhakaran, A. Chandran, A. R. Sreekutty, S. Madesh, R. Pachaiappan, B. O. Almutairi, S. Arokiyaraj, Z. A. Kari, G. Tellez-Isaias, A. Guru and J. Arockiaraj, *Molecules*, 2023, **28**, 5350.

93 N. Qamar, P. John and A. Bhatti, *Int. J. Nanomedicine*, 2020, **Volume 15**, 3497–3509.

View Article Online
DOI: 10.1039/D4NA00644E

Table 1Primer sequence used in RT-PCR

Gene	Forward Primer(5' to 3')	Reverse Primer (5' to 3')	Reference
SOD	GGTCCGCACTTCAACCCTCA	TACCCAGGTCTCCGACGTGT	NCBI: NM_131294.1
CAT	AACTGTGGAAGGAGGGTCGC	CGCTCTCGGTCAAAATGGGC	NCBI: XM_021470442.1
GSR	GATGGGCACCATAGCTAACCC	CATGAGCAGGAAGCAACACCC	NCBI: XM_005169592.4
GPx	AACTACACTCAGCTTGCGGC	TCCGCTTCACTTCCAGGCTC	NCBI: NM_001030070.2
β-actin	AAGCTGTGACCCACCTCACG	GGCTTTGCACATACCGGAGC	NCBI: NM_131031.2